WWPGI; $(QBP1)_2$, SNWKWWPGIFDSNWKWWPGIFD [5,15]. Congo red (CR) was purchased from Division Chroma (Muenster, Germany), and Thioflavin T (ThT) and PGL-135 from Sigma–Aldrich (St. Louis, MO). All peptides were prepared as 100 mM stock solutions, and CR as a 10 mM stock solution in dimethyl sulfoxide. ThT and PGL-135 were directly dissolved in SPR running buffer.

Protein purification. Thioredoxin-polyQ (thio-polyQ) fusion proteins expressed in *Escherichia coli* DH5α were purified using nickel-chelating ProBond Resin columns (Invitrogen, Carlsbad, CA) and anion-exchange chromatography using the Äkta Explore HPLC apparatus equipped with a HiTrap Q sepharose column (GE Healthcare UK Ltd., Little Chalfont, England), as described previously [5]. Protein concentrations were determined by the Lowry method using a DC protein assay kit (Bio-Rad Laboratories, Philadelphia, PA). Thio-polyQ proteins with 62 or 19 glutamines (thio-Q62 or thio-Q19, respectively), or without a polyQ stretch (thio-Q0) were used.

Surface plasmon resonance analysis. The binding kinetics of QBP1-related peptides, CR, ThT, and PGL-135 to the thio-polyQ proteins were determined by SPR analysis using a BIAcore 1000™ system (GE Healthcare). Thio-polyQ was immobilized onto the carboxymethylated dextran matrix on a research grade CM5 sensor chip using an amine coupling kit at a density of 2100–5600 resonance units (RU). Binding experiments were performed using HBS-EP (10 mM Hepes, 0.15 M NaCl, 3 mM EDTA, 0.005% (v/v) surfactant P20, pH 7.4) containing 0.25% dimethyl sulfoxide (QBP1-related peptides and CR) or HBS-EP alone (ThT and PGL-135) as running buffers. Twofold serial dilutions of the peptides and the compounds were injected for 120 s across the thio-polyQ-immobilized sensor surfaces as well as the non-immobilized sensor surface as a reference. The data were analyzed using BIAevaluation software version 4.1 (GE Healthcare). Equilibrium RU values were used to calculate the equilibrium dissociation constant (K_d) fitted by steady-state affinity analysis.

Circular dichroism and native polyacrylamide gel electrophoresis analyses. Thio-Q62 proteins (10 μM) were incubated alone or together with QBP1 (20 μM) or CR (20 μM) in phosphate-buffered saline (PBS, pH 7.5) at 37 °C, and the soluble fractions of thio-Q62 were subjected to circular dichroism (CD) and native polyacrylamide gel electrophoresis (PAGE) analyses. CD spectra of thio-Q62 were measured at 25 °C using a J-700 spectropolarimeter (Jasco, Tokyo, Japan) as described previously [6]. The data are expressed as molar residue ellipticities. Thio-Q62 proteins were also separated by 10% (w/v) PAGE under non-denaturing conditions followed by staining with Coomassie brilliant blue.

Protein aggregation turbidity assay. Aggregate formation of thio-Q62 was assessed by the turbidity assay as described previously [5]. Briefly, thio-Q62 proteins (8 or 10 μM) were incubated alone or together with QBP1-related peptides (20 μM) or CR (20 μM) in PBS at 37 °C, and optical density at 405 nm was measured using a

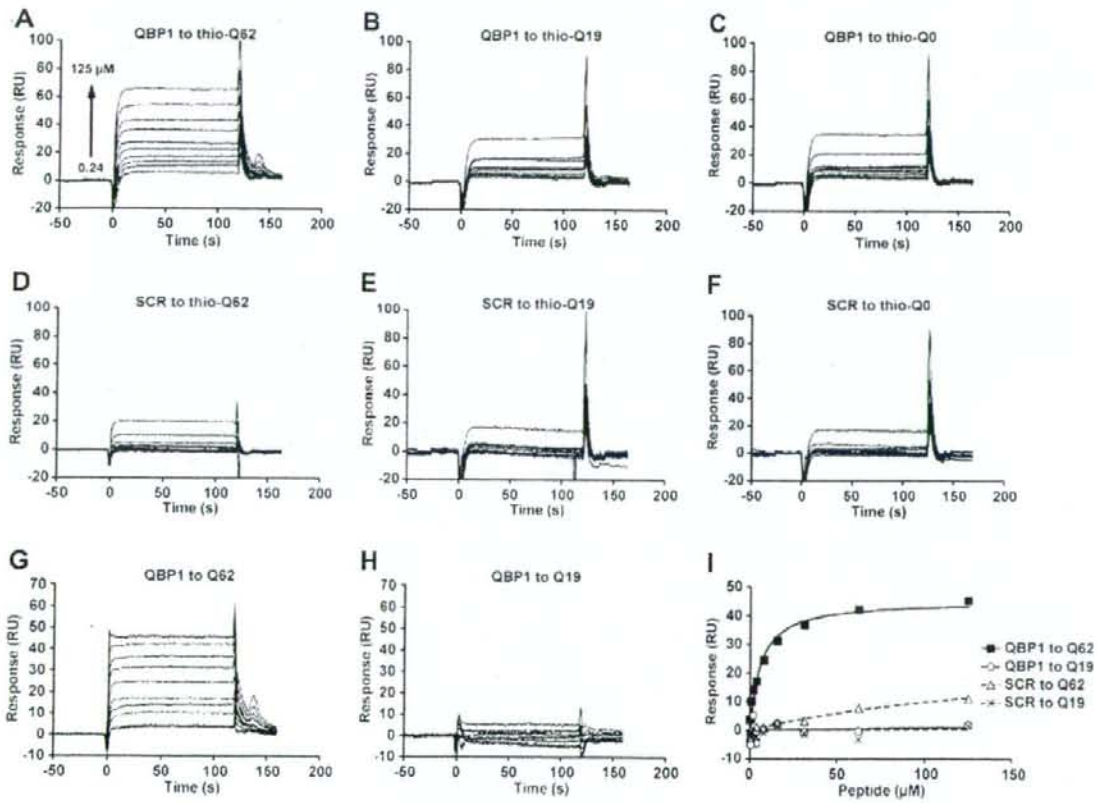

Fig. 1. Detection of specific binding of QBP1 to the expanded polyQ stretch by SPR analysis. (A–F) Typical sensorgrams for binding of QBP1 (A–C) and SCR (D–F) to thio-Q62 (A,D), thio-Q19 (B,E), and thio-Q0 (C,F). Thio-Q62, thio-Q19, and thio-Q0 were immobilized (3600 RU, 4110 RU, and 4200 RU, respectively) onto the sensor surface, and then various concentrations of QBP1 and SCR (0.24–125 μM) were injected. (G,H) Sensorgrams for binding of QBP1 to the polyQ stretches, in which the RU values for thio-Q0 were subtracted from those for thio-Q62 and thio-Q19. (I) Steady-state affinity analyses of binding of QBP1 and SCR to the polyQ stretches.

Spectramax Plus plate reader (Molecular Devices, Sunnyvale, CA). Inhibitory effects of the peptides on thio-Q62 aggregation were evaluated by duration of complete inhibition (>95%) of aggregation.

Results

Detection of specific binding of QBP1 to the expanded polyQ stretch by SPR analysis

To investigate whether SPR analysis could detect specific binding of polyQ aggregation inhibitors to the expanded polyQ stretch, we evaluated the binding affinity of QBP1 to thioredoxin-polyQ (thio-polyQ) proteins with various polyQ-lengths. Various concentrations of QBP1 (0.24–125 μM) were injected across sensor surfaces which were immobilized with thio-Q62, thio-Q19 or thio-Q0 proteins. We found that the RU values for thio-Q62 significantly increase with increasing concentrations of QBP1, while only slight changes were observed both for thio-Q0 and thio-Q19 (Fig. 1A–C). The control peptide SCR, a scrambled sequence of QBP1, also showed only slight changes in its RU values to all the thio-polyQ proteins (Fig. 1D–F), suggesting that QBP1 preferentially binds to the thio-Q62 protein. Upon subtraction of the RU values for thio-Q0 from those for thio-Q62 and thio-Q19, significant binding of QBP1 to the Q62 stretch become more apparent (Fig. 1G and H), suggesting that QBP1 binds specifically to the expanded polyQ stretch. By steady-state affinity analysis, the equilibrium dissociation constant (K_d) for binding of QBP1 to the Q62 stretch was calculated to be 5.7 μM (Fig. 1I and Table 1). These results indicate that SPR analysis successfully and quantitatively detects specific binding of QBP1 to the expanded polyQ stretch.

Table 1
Equilibrium dissociation constants (K_d) for binding of QBP1-related peptides to the Q62 stretch and their inhibitory effects on aggregate formation of thio-Q62.

Peptide	Sequence	K_d (μM)	Duration of complete inhibition (day)
$(QBP1)_2$	SNWKWWPGIFDSNWKWWPGIFD	0.6 ± 0.2	8.1
QBP1	SNWKWWPGIFD	5.7 ± 0.8	5.7
QBP1-C9	--WKWWPGIFD	5.7 ± 1.0	3.6
QBP1-M8	--WKWWPGIF-	4.6 ± 0.7	4.1
QBP1-N9	SNWKWWPGI--	24.0 ± 3.0	1.6
SCR	WPIWSKGNIWF	ND	1.0

WKWWPGIF (underlined) is the minimal active sequence of QBP1 [15]. Variations for K_d values are standard errors. ND, not detected.

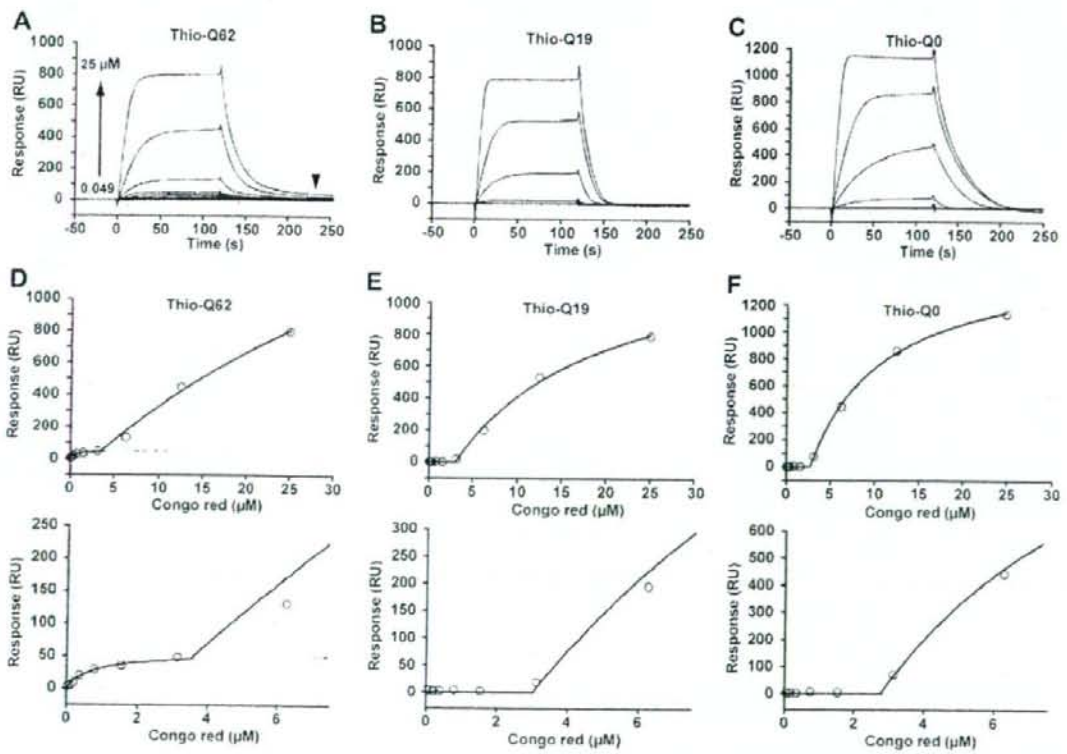

Fig. 2. Non-specific binding of CR to polyQ proteins. (A–C) Typical sensorgrams for binding of CR to thio-Q62 (A), thio-Q19 (B), and thio-Q0 (C). Thio-Q62, thio-Q19, and thio-Q0 were immobilized (5550 RU, 2090 RU, and 3270 RU, respectively) onto the sensor surface, and then various concentrations of CR (0.049–25 μM) were injected. (D–F) Steady-state affinity analyses of CR binding to thio-Q62 (D), thio-Q19 (E), and thio-Q0 (F). Plots of the lower concentration range (indicated by a dotted box in the upper panels) are shown in the lower panels.

Non-specific binding of CR to thio-polyQ proteins independent of their polyQ-length

We next examined the binding specificity of CR, a well-known polyQ aggregation inhibitor [11], to thio-polyQ proteins with various polyQ-lengths by SPR analysis. In contrast to QBP1, the RU values for all of these thio-polyQ proteins dramatically increased with CR concentrations, suggesting that CR non-specifically binds to thio-polyQ proteins independently of the polyQ sequences (Fig. 2A–C). However, steady-state affinity analysis revealed that non-specific binding of CR to all the thio-polyQ proteins was observed only above approximately 3 μM, whereas below 3 μM, the RU values only for thio-Q62 significantly increase with increasing CR concentrations, with apparently distinct kinetics from the above (Fig. 2D–F). The K_d value for binding of CR (below 3 μM) to thio-Q62 was calculated to be 730 nM, while the K_d values for binding of CR (above 3 μM) to the thio-polyQ proteins were calculated to be more than 10 μM. Non-specific binding of CR to thio-polyQ proteins above 3 μM is probably due to the formation of colloidal aggregates at micromolar concentrations as reported previously [13,16]. In addition, CR did not completely dissociate from thio-Q62 even after thorough washing with the running buffer (Fig. 2A, arrowhead), implying that CR binds specifically to the amyloid-like fibrillar aggregates of thio-Q62 formed on the sensor surface at low concentrations [17].

In addition to CR, we also examined the binding specificities of thioflavin T (ThT), an amyloid-staining dye [18], and PGL-135, a polyQ aggregation inhibitor [12], to the thio-polyQ proteins. As shown in Supplementary Fig. 1, both ThT and PGL-135 bound non-specifically to all of the thio-polyQ proteins, suggesting that their binding to thio-polyQ also does not depend on the polyQ sequences.

QBP1 and CR both inhibit polyQ aggregation but through distinct modes of action

The differences in the binding specificities of QBP1 and CR to the thio-polyQ proteins prompted us to investigate their effects on the conformation and aggregation of thio-polyQ. We previously demonstrated by circular dichroism (CD) and native PAGE that thio-Q62 gradually undergoes a conformational transition from an α-helix-dominant structure to a β-sheet-dominant structure upon incubation at 37 °C (Fig. 3A and B), resulting in formation of amyloid-like fibrillar aggregates, which can be assessed by the turbidity assay (Fig. 3C) [6]. We found that both QBP1 and CR effectively inhibit aggregate formation of thio-Q62 upon coincubation (Fig. 3C), consistent with previous studies [5,11]. However, whereas QBP1, which specifically binds to the expanded polyQ stretch, almost completely inhibits the β-sheet conformational transition of thio-Q62 [6], CR showed a much weaker effect (Fig. 3A and B), implying that CR instead inhibits the assembly of β-sheet-transformed polyQ proteins into amyloid-like fibrillar aggregates, consistent with previous studies [7,19]. These results indicate that QBP1 and CR inhibit aggregate formation of thio-polyQ through distinct modes of action, and further imply that specific binding to the expanded polyQ stretch plays a crucial role in inhibition of its toxic conformational transition to a β-sheet.

Binding affinities of polyQ aggregation inhibitors to the expanded polyQ stretch correlate with their inhibitory effects

We next investigated the relationship between the binding affinities of QBP1 and its variants to the expanded polyQ protein and their inhibitory effects on aggregation. We previously identified the minimal active sequence of QBP1 (M8; --WKWWPGIF-) [15]. SPR analyses revealed that the K_d values of QBP1-M8 and

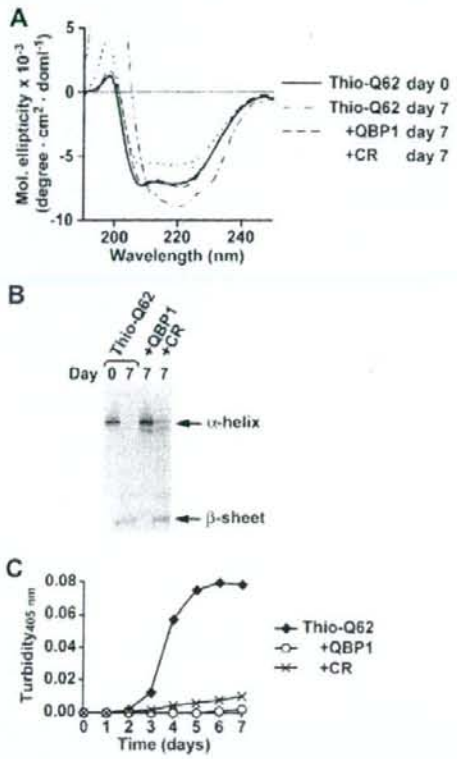

Fig. 3. QBP1 inhibits the conformational transition of the expanded polyQ protein, while CR does not. CD (A), native PAGE (B), and aggregation turbidity assay (C) of thio-Q62 (10 μM) coincubated with QBP1 (20 μM) or CR (20 μM).

QBP1-C9 (--WKWWPGIFD) to the Q62 stretch, which almost fully retain the inhibitory effect on thio-Q62 aggregation, are calculated to be 5.7 and 4.6 μM, respectively, which were almost equal to that of QBP1 (5.7 μM, Table 1). QBP1-N9 (SNWKWWPGI--) lacking the FD at the C-terminus showed a much weaker inhibitory effect on thio-Q62 aggregation than QBP1 (Fig. 4B) and its K_d value to the Q62 stretch is 24.0 μM, correspondingly much higher than that of QBP1 (Fig. 4A and Table 1). On the other hand $(QBP1)_2$, a tandem repeat of QBP1, has the greatest binding affinity to the Q62 stretch (K_d = 0.6 μM) and exhibited the strongest inhibitory effect with more than 8 days of complete inhibition on thio-Q62 aggregation among the QBP1-related peptides (Fig. 4 and Table 1). SCR, which has no significant binding affinity to the Q62 stretch, did not show any inhibitory effects on thio-Q62 aggregation. As shown in Fig. 4C, we found a significant correlation between the K_d values of QBP1-related peptides to the Q62 stretch and duration of complete inhibition of thio-Q62 aggregation (R^2 = 0.89). Taken together, these results suggest that the binding affinities of polyQ aggregation inhibitors to the expanded polyQ stretch predict their inhibitory effects on polyQ aggregation.

Discussion

High-throughput chemical screening has been a useful strategy for the discovery of novel lead compounds for drug development so far. However, this strategy produces common false-positive hits regardless of the various targets of each screening, and these

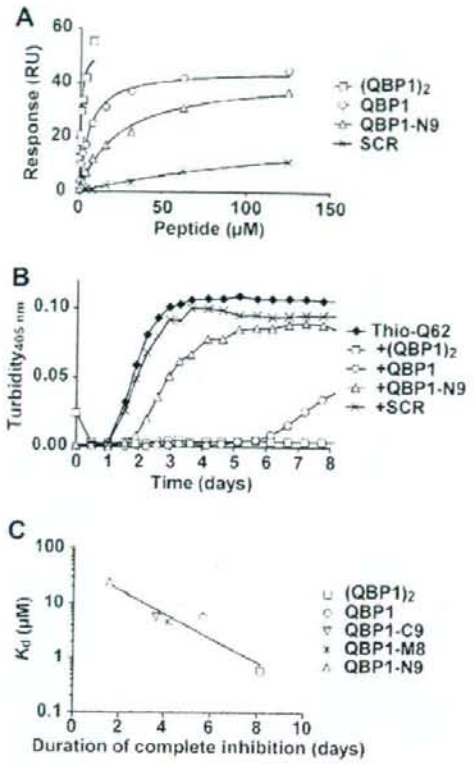

Fig. 4. The binding affinities of QBP1-related peptides to the expanded polyQ stretch correlate with their inhibitory effects on polyQ aggregation. (A) Steady-state affinity analyses of binding of QBP1-related peptides to the Q62 stretch. The K_d values of $(QBP1)_2$, QBP1, and QBP1-N9 to the Q62 stretch were calculated to be 0.6, 5.7, and 24.0 μM, respectively (Table 1). (B) Aggregation turbidity assay of thio-Q62 (8 μM) coincubated with QBP1-related peptides (20 μM). (C) Correlation between the K_d values of QBP1-related peptides to the Q62 stretch and duration of complete inhibition of thio-Q62 aggregation ($R^2 = 0.89$).

non-specific hits include chemical aggregators, which form promiscuous colloidal aggregates [20]. Colloidal aggregates have been reported to physically sequester various unrelated proteins, resulting in non-specific inhibition of enzymatic activity or amyloid fibril formation of prion proteins [13,14]. Notably, CR, which is known to inhibit aggregate formation of various amyloidogenic proteins including polyQ proteins, is also classified as a chemical aggregator [11,14,17]. In this study, we showed that CR as well as ThT and PGL-135 non-specifically binds to thio-polyQ proteins independently of their polyQ-length (Fig. 2 and Supplementary Fig. 1). We further showed that CR does not efficiently inhibit the toxic β-sheet conformational transition of the expanded polyQ protein (Fig. 3), probably because CR binds to polyQ oligomers/aggregates but not specifically to the polyQ monomer. The therapeutic effects of non-specific aggregation inhibitors such as CR and PGL-135 on animal models of the polyQ diseases have been controversial [21–23], probably due to the lack of their ability to inhibit the toxic conformational transition of the expanded polyQ protein. On the other hand, we successfully showed that QBP1 specifically binds to the expanded polyQ stretch (Fig. 1) and inhibits its toxic conformational transition as well as aggregate formation (Fig. 3), and previously showed that QBP1 suppresses polyQ-induced neurodegeneration *in vivo* [8,9]. These data indicate that the SPR technique can distinguish non-specific aggregation inhibitors from specific polyQ aggregation inhibitors, which are expected to exert inhibitory effects on the toxic conformational transition and are thus promising drug candidates without side effects for the polyQ diseases.

The SPR technique is a highly sensitive method for quantitative evaluation of biomolecular interactions, and has been widely applied for chemical screening and characterization [24]. In this study, we showed by SPR analysis that the binding affinities of QBP1-related peptides to the expanded polyQ stretch correlate with their inhibitory effects on polyQ aggregation (Fig. 4 and Table 1). Previous studies also reported significant correlations between the binding affinities of anti-amyloid compounds and their inhibitory effects [25,26]. Taken together, we conclude that SPR is a powerful technique to predict the therapeutic efficacy of aggregation inhibitors and can be applied for the screening of not only polyQ aggregation inhibitors but also other protein aggregation inhibitors, as therapeutic candidates for the other neurodegenerative diseases, such as Alzheimer disease and prion diseases.

Several anti-polyQ antibodies have been established so far, including 1C2 [27], 3B5H10 [28], MW1, and MW2 [29], which preferentially bind to the expanded polyQ protein. However, the 1C2-Fab and MW1 Fv fragment were recently shown by SPR analysis to exhibit similar binding affinities for expanded and normal polyQ stretches [30,31], indicating that these bivalent antibodies simply recognize an increased number of glutamine epitopes rather than the conformational difference. On the other hand, we successfully detected the specific binding of QBP1 to thio-Q62, but not to thio-Q19 (Fig. 1), implying that QBP1 may specifically recognize the toxic β-sheet conformation of the expanded polyQ stretch. So far, QBP1 is the only molecule which has been shown to specifically bind to the expanded polyQ stretch and to inhibit its toxic β-sheet conformational transition, resulting in suppression of polyQ-induced neurodegeneration *in vivo* [6,8,9]. Further studies to understand the mechanisms involved in the specific recognition of the toxic polyQ conformation by QBP1 will help us to develop therapeutic molecules for the polyQ diseases.

Acknowledgments

We thank Yvon Trottier, Fabrice A.C. Klein, James R. Burke, and Warren J. Strittmatter for helpful discussions, and Chiyomi Ito for technical assistance. This work was supported in part by Grants-in-Aid for Scientific Research on Priority Areas (Y.N.; Research on Pathomechanisms of Brain Disorders, Protein Community, Water and Biomolecules, and Transportsome) from the Ministry of Education, Culture, Sports, Science, and Technology, Japan; by a Grant-in-Aid for the Research Committee for Ataxic Diseases (Y.N.) from the Ministry of Health, Labor and Welfare, Japan; by Grants-in-Aid for Scientific Research (B) (Y.N. and T.I.) from the Japan Society for the Promotion of Science, Japan; and by grants from the Japan Foundation for Applied Enzymology (T.I.) and Osaka Prefecture (T.I.).

Appendix A. Supplementary data

Supplementary data associated with this article can be found, in the online version, at doi:10.1016/j.bbrc.2008.11.094.

References

[1] H.T. Orr, H.Y. Zoghbi, Trinucleotide repeat disorders, Annu. Rev. Neurosci. 30 (2007) 575–621.
[2] J. Shao, M.I. Diamond, Polyglutamine diseases: emerging concepts in pathogenesis and therapy, Hum. Mol. Genet. 16 (Spec. No. 2) (2007) R115–R123.
[3] C.A. Ross, M.A. Poirier, Protein aggregation and neurodegenerative disease, Nat. Med. 10 (Suppl.) (2004) S10–S17.

[4] Y. Nagai, H.A. Popiel, Conformational changes and aggregation of expanded polyglutamine proteins as therapeutic targets of the polyglutamine diseases: exposed β-sheet hypothesis, Curr. Pharm. Des., in press.
[5] Y. Nagai, T. Tucker, H. Ren, et al., Inhibition of polyglutamine protein aggregation and cell death by novel peptides identified by phage display screening, J. Biol. Chem. 275 (2000) 10437–10442.
[6] Y. Nagai, T. Inui, H.A. Popiel, et al., A toxic monomeric conformer of the polyglutamine protein, Nat. Struct. Mol. Biol. 14 (2007) 332–340.
[7] Y. Takahashi, Y. Okamoto, H.A. Popiel, et al., Detection of polyglutamine protein oligomers in cells by fluorescence correlation spectroscopy, J. Biol. Chem. 282 (2007) 24039–24048.
[8] Y. Nagai, N. Fujikake, K. Ohno, et al., Prevention of polyglutamine oligomerization and neurodegeneration by the peptide inhibitor QBP1 in *Drosophila*, Hum. Mol. Genet. 12 (2003) 1253–1259.
[9] H.A. Popiel, Y. Nagai, N. Fujikake, et al., Protein transduction domain-mediated delivery of QBP1 suppresses polyglutamine-induced neurodegeneration *in vivo*, Mol. Ther. 15 (2007) 303–309.
[10] H.A. Popiel, Y. Nagai, N. Fujikake, et al., Delivery of the aggregate inhibitor peptide QBP1 into the mouse brain using PTDs and its therapeutic effect on polyglutamine disease mice, Neurosci. Lett. 449 (2009) 87–92.
[11] V. Heiser, E. Scherzinger, A. Boeddrich, et al., Inhibition of huntingtin fibrillogenesis by specific antibodies and small molecules: implications for Huntington's disease therapy, Proc. Natl. Acad. Sci. USA 97 (2000) 6739–6744.
[12] V. Heiser, S. Engemann, W. Brocker, et al., Identification of benzothiazoles as potential polyglutamine aggregation inhibitors of Huntington's disease by using an automated filter retardation assay, Proc. Natl. Acad. Sci. USA 99 (Suppl. 4) (2002) 16400–16406.
[13] S.L. McGovern, E. Caselli, N. Grigorieff, et al., A common mechanism underlying promiscuous inhibitors from virtual and high-throughput screening, J. Med. Chem. 45 (2002) 1712–1722.
[14] B.Y. Feng, B.H. Toyama, H. Wille, et al., Small-molecule aggregates inhibit amyloid polymerization, Nat. Chem. Biol. 4 (2008) 197–199.
[15] H. Ren, Y. Nagai, T. Tucker, et al., Amino acid sequence requirements of peptides that inhibit polyglutamine–protein aggregation and cell death, Biochem. Biophys. Res. Commun. 288 (2001) 703–710.
[16] A.M. Giannetti, B.D. Koch, M.F. Browner, Surface plasmon resonance based assay for the detection and characterization of promiscuous inhibitors, J. Med. Chem. 51 (2008) 574–580.
[17] P. Frid, S.V. Anisimov, N. Popovic, Congo red and protein aggregation in neurodegenerative diseases, Brain Res. Rev. 53 (2007) 135–160.
[18] H. LeVine 3rd, Quantification of β-sheet amyloid fibril structures with thioflavin T, Methods Enzymol. 309 (1999) 274–284.
[19] M.A. Poirier, H. Li, J. Macosko, et al., Huntingtin spheroids and protofibrils as precursors in polyglutamine fibrilization, J. Biol. Chem. 277 (2002) 41032–41037.
[20] G.M. Rishton, Nonleadlikeness and leadlikeness in biochemical screening, Drug Discov. Today 8 (2003) 86–96.
[21] N.I. Wood, P.N. Pallier, J. Wanderer, et al., Systemic administration of Congo red does not improve motor or cognitive function in R6/2 mice, Neurobiol. Dis. 25 (2007) 342–353.
[22] E. Hockly, J. Tse, A.L. Barker, et al., Evaluation of the benzothiazole aggregation inhibitors riluzole and PGL-135 as therapeutics for Huntington's disease, Neurobiol. Dis. 21 (2006) 228–236.
[23] I. Sanchez, C. Mahlke, J. Yuan, Pivotal role of oligomerization in expanded polyglutamine neurodegenerative disorders, Nature 421 (2003) 373–379.
[24] W. Huber, A new strategy for improved secondary screening and lead optimization using high-resolution SPR characterization of compound-target interactions, J. Mol. Recognit. 18 (2005) 273–281.
[25] S. Kawatake, Y. Nishimura, S. Sakaguchi, et al., Surface plasmon resonance analysis for the screening of anti-prion compounds, Biol. Pharm. Bull. 29 (2006) 927–932.
[26] C.W. Cairo, A. Strzelec, R.M. Murphy, et al., Affinity-based inhibition of β-amyloid toxicity, Biochemistry (Mosc.) 41 (2002) 8620–8629.
[27] Y. Trottier, Y. Lutz, G. Stevanin, et al., Polyglutamine expansion as a pathological epitope in Huntington's disease and four dominant cerebellar ataxias, Nature 378 (1995) 403–406.
[28] C. Peters-Libeu, Y. Newhouse, P. Krishnan, et al., Crystallization and diffraction properties of the Fab fragment of 3B5H10, an antibody specific for disease-causing polyglutamine stretches, Acta Crystallogr. Sect. F. Struct. Biol. Cryst. Commun. 61 (2005) 1065–1068.
[29] J. Ko, S. Ou, P.H. Patterson, New anti-huntingtin monoclonal antibodies: implications for huntingtin conformation and its binding proteins, Brain Res. Bull. 56 (2001) 319–329.
[30] F.A. Klein, A. Pastore, L. Masino, et al., Pathogenic and non-pathogenic polyglutamine tracts have similar structural properties: towards a length-dependent toxicity gradient, J. Mol. Biol. 371 (2007) 235–244.
[31] P. Li, K.E. Huey-Tubman, T. Gao, et al., The structure of a polyQ–anti-polyQ complex reveals binding according to a linear lattice model, Nat. Struct. Mol. Biol. 14 (2007) 381–387.

Bioorganic & Medicinal Chemistry 17 (2009) 1259–1263

Contents lists available at ScienceDirect

Bioorganic & Medicinal Chemistry

journal homepage: www.elsevier.com/locate/bmc

Structure–activity relationship study on polyglutamine binding peptide QBP1

Kenji Tomita [a,†], H. Akiko Popiel [b,†,‡], Yoshitaka Nagai [b,*,‡], Tatsushi Toda [b], Yuji Yoshimitsu [a], Hiroaki Ohno [a], Shinya Oishi [a,*], Nobutaka Fujii [a]

[a] Graduate School of Pharmaceutical Sciences, Kyoto University, Sakyo-ku, Kyoto 606-8501, Japan
[b] Graduate School of Medicine, Osaka University, Suita, Osaka 565-0871, Japan

ARTICLE INFO

Article history:
Received 14 November 2008
Revised 6 December 2008
Accepted 9 December 2008
Available online 24 December 2008

Keywords:
QBP1
Polyglutamine diseases
Structure–activity relationship study

ABSTRACT

Aggregation and deposition of expanded polyglutamine proteins in the brain cause neurodegenerative diseases including Huntington disease. This pathogenic process is suppressed and delayed in the presence of polyglutamine binding peptide 1 (QBP1), which we previously identified as an undecapeptide binding to pathogenic polyglutamine proteins from phage display peptide libraries. In this paper, a structure–activity relationship study on QBP1 was conducted to determine the pharmacophores for inhibition of polyglutamine aggregation. Furthermore, a truncation study identified an octapeptide as the minimum structure for suppressing aggregation of polyglutamine proteins, which is equipotent to the parent undecapeptide QBP1.

1. Introduction

Conformational neurodegenerative diseases, such as Alzheimer and Parkinson disease, are caused by the abnormal accretion and deposition of misfolded proteins in the central nervous system.[1] Among them, the polyglutamine (polyQ) diseases, including Huntington disease, various types of spinocerebellar ataxia, spinobulbar muscular atrophy, and dentatorubral pallidoluysian atrophy, are caused by proteins containing an expanded polyQ repeat (more than 40 glutamines) encoded by a common mutation of a consecutive CAG trinucleotide repeat expansion.[2,3] In the pathogenesis of the polyQ diseases, a conformational change of the polyQ stretch caused by its pathogenic expansion is thought to be a key step leading to aggregation of the polyQ protein, which eventually results in its visible deposition as inclusion bodies inside affected neurons. Although the mechanism of polyQ aggregate formation has not been revealed, our recent study suggests that a β-sheet conformational transition of the expanded polyQ protein monomer precedes its assembly into β-sheet-rich amyloid-like fibrils.[4,5] To date, several inhibitors of polyQ protein aggregation have been identified. They include small peptides binding to the polyQ stretch,[6] intracellular antibodies (intrabodies) against the polyQ proteins,[7,8] molecular chaperones targeting misfolded proteins,[9–11] and small chemical compounds.[12–15] In spite of these findings, there are currently no effective therapies clinically available for polyQ disease patients.

We previously reported six novel undecapeptides binding to the expanded polyQ stretch, which were identified from combinatorial peptide phage display libraries (Table 1).[16] Among them, polyglutamine binding peptide 1 (QBP1) binds to pathologic-length polyQ more selectively compared to the other QBPs.[16] The inhibition of polyQ protein oligomerization by QBP1 is significantly observed not only against the purified polyQ protein but also that in cells.[17] A tandem repeat of QBP1, co-expressed with pathogenic polyQ proteins, rescues polyQ-induced compound eye generation and premature death in *Drosophila melanogaster*.[18] Furthermore, protein transduction domain (PTD)[19–21]-conjugates of QBP1 suppress polyQ-induced neurodegeneration in animal models.[22,23] Although the mechanisms of inhibition of polyQ protein aggregation by QBP1 has not been completely revealed, our recent research suggests that QBP1 prevents the toxic β-sheet conformational transition of the pathologic-length polyQ protein monomer as well as its subsequent oligomer formation.[4,5] These results indicate that QBP1 is a promising lead compound for preventing disease onset and for slowing progression of the polyQ diseases. Our previous work on several QBP1 derivatives demonstrated that truncation of two N-terminal (Ser1 and Asn2) and one C-terminal (Asp11) amino acid residue is tolerable,[24] and that a positively charged amino acid adjacent to the Trp residue is conserved among QBPs identified from phage display screening (Table 1). These data could be useful for development of novel inhibitors; however, a more comprehensive investigation is needed for elucidation of the structural requirements of QBP1. In this study, we conducted

* Corresponding authors. Tel.: +81 75 753 4551; fax: +81 75 753 4570 (S.O.).
E-mail addresses: nagai@ncnp.go.jp (Y. Nagai), soishi@pharm.kyoto-u.ac.jp (S. Oishi).

† These authors contributed equally to this work.

‡ Present address: National Institute of Neuroscience, National Center of Neurology and Psychiatry, Kodaira, Tokyo 187-8502, Japan.

0968-0896/$ - see front matter © 2008 Elsevier Ltd. All rights reserved.
doi:10.1016/j.bmc.2008.12.018

Table 1
Polyglutamine binding peptides (QBPs) identified from phage display peptide libraries

Peptide	Sequence
QBP1	Ac-Ser-Asn-Trp-Lys-Trp-Trp-Pro-Gly-Ile-Phe-Asp-NH_2
QBP2	Ac-His-Trp-Trp-Arg-Ser-Trp-Tyr-Ser-Asp-Ser-Val-NH_2
QBP3	Ac-His-Glu-Trp-His-Trp-Trp-His-Gln-Glu-Ala-Ala-NH_2
QBP4	Ac-Trp-Gly-Leu-Glu-His-Phe-Ala-Gly-Asn-Lys-Arg-NH_2
QBP5	Ac-Trp-Trp-Arg-Trp-Asn-Trp-Ala-Thr-Pro-Val-Asp-NH_2
QBP6	Ac-Trp-His-Asn-Tyr-Phe-His-Trp-Trp-Gln-Asp-Thr-NH_2

alanine- and D-amino acid scanning of QBP1 to identify the pharmacophores for inhibitory activity against oligomerization of the polyQ protein and to investigate the importance of stereochemistry of each amino acid residue, respectively. Moreover, we examined a series of N- and/or C-terminal truncated QBP1 derivatives to determine the minimum sequence for inhibition of polyQ aggregation.

2. Results and discussion

2.1. Synthesis of QBP1 derivatives

All peptide chains were constructed by standard Fmoc-based solid phase peptide synthesis (Fmoc-SPPS) on Rink-amide resin. N-Terminal acetylation was operated by treatment with Ac_2O in the presence of *i*-Pr_2NEt. Final deprotection and cleavage from the resin with the cocktail, TFA/thioanisole/*m*-cresol/1,2-ethanedithiol/H_2O (80:5:5:5:5), followed by RP-HPLC purification afforded the peptides as TFA salts. All peptides were identified with MALDI-TOF-MS and the purity was more than 95% by analytical HPLC.

2.2. Biological evaluation of synthetic peptides

The bioactivity of synthesized peptides was evaluated based on the inhibitory potency against aggregation of a thioredoxin-conjugated polyQ protein (62-mer), which has advantages of high solubility, possibility of high concentration expression in *Escherichia coli* (*E. coli*), and easy purification.[25] Turbidity of this polyQ protein was traced by measuring at 405 nm. PolyQ protein aggregation increases in a time- and concentration-dependent manner and eventually reaches a plateau.[16] Relative inhibitory activity (% inhibition) induced by 20 μM of each QBP1 derivative was evaluated in duplicate by comparison to the plateau level (0% inhibition). Furthermore, IC_{50} values were calculated for potent inhibitors, exerting more than 50% inhibition at 20 μM.

2.3. Structure–activity relationships studies on QBP1

2.3.1. Alanine scanning of QBP1

In order to identify pharmacophores for the prevention of polyQ protein aggregation, each amino acid residue of QBP1 was substituted with alanine (Table 2). Replacement of Trp3, Trp5, Trp6, Ile9 and Phe10 resulted in a significant decrease of inhibitory activities (peptides **3**, **5**, **6**, **9** and **10**; less than 20% inhibition at 20 μM). This result indicates that functional groups of these five residues are involved in inhibition of polyQ protein aggregation through direct or indirect interaction. All QBPs identified from phage display libraries[16] possess more than two aromatic amino acid residues, in which at least one is a tryptophan residue (Table 1). Based on this result, aromatic groups, especially indole rings of tryptophan, might contribute to the biological activity.

On the other hand, alanine-substitutions of Ser1, Asn2, Lys4, Pro7, Gly8 and Asp11 are tolerable (peptides **1**, **2**, **4**, **7**, **8** and **11**; IC_{50} < 20 μM). Similar results were obtained for Lys4 and Pro7 substitutions in our previous study, which showed that each of them can be replaced with valine.[24] All hydrophilic functional groups of the side chain, hydroxy (Ser1), primary amide (Asn2), amine (Lys4) and carboxylic acid (Asp11), are not required for inhibition of polyQ aggregation. Taken together with the above result indicating that hydrophobic amino acid residues are pharmacophores, it is conceivable that hydrophobicity of QBP1 is important for its interaction with polyQ proteins. This is supported by the result that the C-terminal tetrapeptide (Gly-Ile-Phe-Asp) is replaceable with a tryptophan-rich tetrapeptide (Trp-Lys-Trp-Trp) without the loss of inhibitory activity.[24] Although proline and glycine are often ob-

Table 2
Alanine and D-amino acid scanning of QBP1

Peptide	Sequence	% Inhibition	IC_{50} (μM)
QBP1	Ac-Ser-Asn-Trp-Lys-Trp-Trp-Pro-Gly-Ile-Phe-Asp-NH_2	76.7	5.0
Alanine scanning			
1	Ac-*Ala*-Asn-Trp-Lys-Trp-Trp-Pro-Gly-Ile-Phe-Asp-NH_2	78.2	6.3
2	Ac-Ser-*Ala*-Trp-Lys-Trp-Trp-Pro-Gly-Ile-Phe-Asp-NH_2	82.2	4.3
3	Ac-Ser-Asn-*Ala*-Lys-Trp-Trp-Pro-Gly-Ile-Phe-Asp-NH_2	−4.0	–[a]
4	Ac-Ser-Asn-Trp-*Ala*-Trp-Trp-Pro-Gly-Ile-Phe-Asp-NH_2	78.2	8.5
5	Ac-Ser-Asn-Trp-Lys-*Ala*-Trp-Pro-Gly-Ile-Phe-Asp-NH_2	−5.4	–[a]
6	Ac-Ser-Asn-Trp-Lys-Trp-*Ala*-Pro-Gly-Ile-Phe-Asp-NH_2	−10.4	–[a]
7	Ac-Ser-Asn-Trp-Lys-Trp-Trp-*Ala*-Gly-Ile-Phe-Asp-NH_2	58.9	10.0
8	Ac-Ser-Asn-Trp-Lys-Trp-Trp-Pro-*Ala*-Ile-Phe-Asp-NH_2	64.9	11.5
9	Ac-Ser-Asn-Trp-Lys-Trp-Trp-Pro-Gly-*Ala*-Phe-Asp-NH_2	9.9	–[a]
10	Ac-Ser-Asn-Trp-Lys-Trp-Trp-Pro-Gly-Ile-*Ala*-Asp-NH_2	11.4	–[a]
11	Ac-Ser-Asn-Trp-Lys-Trp-Trp-Pro-Gly-Ile-Phe-*Ala*-NH_2	67.8	15.6
D-Amino acid scanning			
12	Ac-D-*Ser*-Asn-Trp-Lys-Trp-Trp-Pro-Gly-Ile-Phe-Asp-NH_2	83.2	4.4
13	Ac-Ser-D-*Asn*-Trp-Lys-Trp-Trp-Pro-Gly-Ile-Phe-Asp-NH_2	80.7	4.5
14	Ac-Ser-Asn-D-*Trp*-Lys-Trp-Trp-Pro-Gly-Ile-Phe-Asp-NH_2	41.1	–[a]
15	Ac-Ser-Asn-Trp-D-*Lys*-Trp-Trp-Pro-Gly-Ile-Phe-Asp-NH_2	9.9	–[a]
16	Ac-Ser-Asn-Trp-Lys-D-*Trp*-Trp-Pro-Gly-Ile-Phe-Asp-NH_2	6.4	–[a]
17	Ac-Ser-Asn-Trp-Lys-Trp-D-*Trp*-Pro-Gly-Ile-Phe-Asp-NH_2	8.4	–[a]
18	Ac-Ser-Asn-Trp-Lys-Trp-Trp-D-*Pro*-Gly-Ile-Phe-Asp-NH_2	25.7	–[a]
19	Ac-Ser-Asn-Trp-Lys-Trp-Trp-Pro-D-*Ala*-Ile-Phe-Asp-NH_2	16.3	–[a]
20	Ac-Ser-Asn-Trp-Lys-Trp-Trp-Pro-Gly-D-*Ile*-Phe-Asp-NH_2	33.2	–[a]
21	Ac-Ser-Asn-Trp-Lys-Trp-Trp-Pro-Gly-Ile-D-*Phe*-Asp-NH_2	65.3	>20.0
22	Ac-Ser-Asn-Trp-Lys-Trp-Trp-Pro-Gly-Ile-Phe-D-*Asp*-NH_2	77.2	5.0

[a] Not tested.

Table 3
Sequence and biological activity of QBP1 and its truncated analogs

Peptide	Sequence	% Inhibition	IC_{50} (μM)
QBP1	Ac-Ser-Asn-Trp-Lys-Trp-Trp-Pro-Gly-Ile-Phe-Asp-NH_2	76.7	5.0
N-Terminal truncation			
23	Ac-Asn-Trp-Lys-Trp-Trp-Pro-Gly-Ile-Phe-Asp-NH_2	78.2	5.0
24	Ac-Trp-Lys-Trp-Trp-Pro-Gly-Ile-Phe-Asp-NH_2	81.2	2.9
25	Ac-Lys-Trp-Trp-Pro-Gly-Ile-Phe-Asp-NH_2	5.4	–[a]
26	Ac-Trp-Trp-Pro-Gly-Ile-Phe-Asp-NH_2	5.0	–[a]
C-Terminal truncation			
27	Ac-Ser-Asn-Trp-Lys-Trp-Trp-Pro-Gly-Ile-Phe-NH_2	57.4	14.6
28	Ac-Ser-Asn-Trp-Lys-Trp-Trp-Pro-Gly-Ile-NH_2	7.4	–[a]
29	Ac-Ser-Asn-Trp-Lys-Trp-Trp-Pro-Gly-NH_2	5.9	–[a]
30	Ac-Ser-Asn-Trp-Lys-Trp-Trp-Pro-NH_2	11.4	–[a]
NC-Terminal truncation			
31	Ac-Trp-Lys-Trp-Trp-Pro-Gly-Ile-Phe-NH_2	85.6	3.6

[a] Not tested.

served in secondary structures of many bioactive peptides,[26] the substitutions of these amino acid residues in QBP1 with alanine are tolerable, which suggests that they are not involved in the stabilization of a turn or helix substructure. However, removal of Pro7 led to the significant loss of inhibitory activity,[24] indicating that Pro7 works as a spacer between pharmacophores in QBP1.

2.3.2. D-Amino acid scanning of QBP1

Next, D-amino acid scanning of QBP1 was performed in order to explore the importance of stereochemistry of each amino acid residue in QBP1 (Table 2). D-Amino acids can stabilize or destabilize some secondary structures such as β-turn and α-helix conformations, which are often observed as interactive surfaces in bioactive peptides and proteins.[26] The chirality inversion of each residue in the N- or C-terminal region (Ser1, Asn2, Phe10 and Asp11) retained the inhibitory activity (more than 60% inhibition at 20 μM). On the other hand, significantly less bioactivity was observed in the epimeric peptides with a substitution in the internal region (Trp3 to Ile9; less than 50% inhibition at 20 μM), especially from Lys4 to Trp6 (less than 10% inhibition at 20 μM). Although side chain functional groups of Lys4 and Pro7 were not required for inhibition of polyQ aggregation according to the above alanine-scanning study, their (*S*)-configurations are important for the potent inhibitory activity. The potency of peptide **19** (16.3% inhibition at 20 μM) having D-alanine at the original Gly8 position of QBP1 was significantly lower than the L-alanine-substituted congener **8** (64.9% inhibition at 20 μM). Taken together, substitution with D-amino acid residues in QBP1 is disfavored, and the effect of stereochemistry is dependent on the position of the amino acid residue. The internal region is more sensitive to chirality inversion compared to the terminal regions. These results imply that the substitution of D-amino acid disturbs the active conformation of QBP1, although circular dichroism (CD) analysis did not suggest a stabilized secondary structure of QBP1 and any conformational differences between QBP1 and peptides **12**–**22** (see Supplementary data).

2.3.3. Truncated QBP1 analogs

Next, truncated analogs of QBP1 were evaluated to identify the minimum structure for inhibition of polyQ aggregation and to reduce its molecular size (Table 3), which could help towards development of novel low-molecular-weight inhibitors for polyQ aggregation. Initially, we removed N- and C-terminal amino acid residues, respectively. Among the N-terminally truncated analogs **23**–**26**, while N-terminal Ser1- **23** and Ser1-Asn2 dipeptide-truncated **24** analogs exerted anti-aggregation activity (78.2% and 81.2% inhibition at 20 μM, respectively), loss of activity was observed by removal of the N-terminal tripeptide and tetrapeptide containing Trp3 and Lys4 (peptides **25** and **26**, 5.4% and 5.0% inhibition at 20 μM, respectively). This observation is compatible with the result of alanine scanning (Table 1, peptide **3**), which showed that the indole ring of Trp3 is required for binding to the polyQ protein. In the C-terminal truncation, although removal of the C-terminal Asp11 residue was tolerable for maintenance of inhibitory activity (peptide **27**, 57.4% inhibition at 20 μM), the other C-terminally truncated analogs **28**–**30** showed significantly lower inhibitory activity (<20% inhibition at 20 μM). This may be caused by the loss of Ile9 and Phe10, which are also indispensable amino acid residues like Trp3 (Table 1, peptides **10**, **11**). Based on the above results, the octapeptide analog **31** equipotent (IC_{50} = 3.6 μM) to the parent peptide QBP1 (IC_{50} = 5.0 μM) was obtained. This octapeptide **31** seems to be the minimum peptide exerting inhibitory activity against aggregation of polyQ proteins.[24]

3. Conclusion

We conducted a structure–activity relationship study on QBP1 for inhibition of polyQ aggregation. Trp3, Trp5, Trp6, Ile9 and Phe10 were identified as pharmacophores for anti-aggregation of polyQ proteins through alanine-scanning. D-Amino acid scanning showed the importance of (*S*)-stereochemistry of each residue. Although this result may suggest the existence of a specific active conformation of QBP1, further investigation is required for its identification. Moreover, combination of the N- and C-terminal truncation studies identified the minimum octapeptide structure of the polyQ aggregation inhibitor, which includes five indispensable amino acids identified by alanine scanning. The information from the present study will be useful not only for the development of novel low-molecular-weight agents binding to polyQ proteins but also for elucidation of the mechanism of anti-polyQ aggregation activity.

4. Experimental

4.1. General procedure for preparation of peptides

The protected peptide-resin was manually constructed using Fmoc-based solid-phase synthesis on Novasyn® TGR resin (0.26 mmol/g, 190 mg, 0.05 mmol). *t*-Bu ester for Asp, *t*-Bu for Ser, Boc for Lys, and Trt for Asn were employed for side-chain protection. Fmoc-protected amino acid derivatives (0.15 mmol, 3.0 equiv) were successively condensed using *N*,*N*′-diisopropylcarbodiimide (DIC; 23 μL, 0.15 mmol, 3.0 equiv) in the presence of *N*-hydroxybenzotriazole monohydrate (HOBt·H_2O; 23 mg, 0.15 mmol, 3.0 equiv). Completion of each coupling reaction was ascer-

Table 4
Characterization data of the synthetic peptides

Peptide	Yield (%)	$[\alpha]_D$ (CH_3OH)	c (g/dL)	Temp. (°C)	Formula	MALDI-TOF	
						Found	Calculated
1	26	−31.5	0.15	28	$C_{74}H_{93}N_{17}O_{15}Na$	1482.6929	1482.9128
2	27	−31.8	0.16	28	$C_{73}H_{93}N_{16}O_{15}$	1433.7001	1433.5104
3	33	−30.9	0.12	29	$C_{68}H_{89}N_{16}O_{16}$	1361.6637	1361.5050
4	18	−24.0	0.11	29	$C_{71}H_{86}N_{16}O_{16}Na$	1441.6300	1441.5424
5	25	−26.5	0.11	29	$C_{66}H_{89}N_{16}O_{16}$	1361.6637	1361.6861
6	20	−25.7	0.11	29	$C_{66}H_{89}N_{16}O_{16}$	1361.6637	1361.6795
7	20	+8.7	0.10	29	$C_{72}H_{92}N_{17}O_{16}$	1450.6903	1450.6702
8	17	−25.5	0.12	29	$C_{75}H_{95}N_{17}O_{16}Na$	1512.7035	1512.7551
9	30	−35.7	0.10	29	$C_{71}H_{88}N_{17}O_{16}$	1434.6590	1434.6856
10	34	−39.2	0.11	28	$C_{68}H_{80}N_{17}O_{16}$	1400.6746	1400.6846
11	43	−29.5	0.11	28	$C_{73}H_{93}N_{17}O_{14}Na$	1454.6980	1454.5867
12	26	−21.3	0.16	28	$C_{74}H_{94}N_{17}O_{16}$	1476.7059	1476.7697
13	25	−39.9	0.11	28	$C_{74}H_{94}N_{17}O_{16}$	1476.7059	1476.7053
14	23	−37.3	0.10	27	$C_{74}H_{94}N_{17}O_{16}$	1476.7059	1476.6704
15	13	−33.7	0.13	27	$C_{74}H_{94}N_{17}O_{16}$	1476.7059	1476.4467
16	12	−35.3	0.15	27	$C_{74}H_{94}N_{17}O_{16}$	1476.7059	1476.4638
17	23	−47.2	0.13	27	$C_{74}H_{94}N_{17}O_{16}$	1476.7059	1476.5763
18	26	−52.4	0.12	27	$C_{74}H_{94}N_{17}O_{16}$	1476.7059	1476.5108
19	15	−40.2	0.13	28	$C_{75}H_{96}N_{17}O_{16}$	1490.7216	1490.4514
20	29	−29.2	0.12	28	$C_{74}H_{93}N_{17}O_{16}Na$	1498.6878	1498.3904
21	35	−41.4	0.15	28	$C_{74}H_{94}N_{17}O_{16}$	1476.7059	1476.3140
22	15	−40.8	0.12	28	$C_{74}H_{93}N_{17}O_{16}Na$	1498.6878	1498.3625
23	26	−47.0	0.14	28	$C_{71}H_{88}N_{16}O_{14}Na$	1411.6558	1411.6332
24	25	−35.7	0.14	29	$C_{67}H_{82}N_{14}O_{12}Na$	1297.6129	1297.6704
25	19	−50.0	0.13	28	$C_{56}H_{72}N_{12}O_{11}Na$	1111.5336	1111.6064
26	12	−33.5	0.11	28	$C_{50}H_{60}N_{10}O_{10}Na$	983.4386	983.2122
27	39	−42.2	0.20	27	$C_{70}H_{88}N_{16}O_{13}$	1361.6790	1361.7289
28	27	−25.6	0.15	27	$C_{61}H_{80}N_{15}O_{12}$	1214.6106	1214.5966
29	48	−42.0	0.13	28	$C_{55}H_{69}N_{14}O_{11}$	1101.5265	1101.5122
30	32	−44.4	0.14	28	$C_{53}H_{68}N_{13}O_{10}$	1044.5050	1044.4267
31	13	−34.6	0.12	28	$C_{63}H_{78}N_{13}O_9$	1160.6040	1160.5685

tained using the Kaiser ninhydrin test.[27] The Fmoc-protecting group was removed by treating the resin with a DMF/piperidine solution (80/20, v/v). After removal of Fmoc protection of the N-terminal amino acid residue, the amino group was reacted with Ac_2O (40 μL, 0.50 mmol, 10.0 equiv) in the presence of *i*-Pr_2NEt (44 μL, 0.25 mmol, 5.0 equiv). The resulting protected resin was treated with TFA/thioanisole/*m*-cresol/1,2-ethandithiol/H_2O (5 mL; 80:5:5:5:5) at room temperature for 2 h. After removal of the resin by filtration, the filtrate was poured into ice-cold dry diethyl ether (40 mL). The resulting powder was collected by centrifugation and then washed three times with ice-cold dry diethyl ether (3 × 40 mL). The crude product was purified by preparative RP-HPLC on a Cosmosil 5C18-ARII preparative column (Nacalai Tesque, 20 × 250 mm) and a Shimadzu LC-6AD (Shimadzu corporation, Ltd.) in an isocratic mode of CH_3CN solution containing 0.1% (v/v) TFA at a flow rate of 10 mL/min to afford the desired peptide as a colorless powder. All peptides were characterized by MALDI-TOF-MS (AXIMA-CFR plus, Shimadzu, Kyoto, Japan, Table 4) and the purity was calculated as >95% by HPLC on a Cosmosil 5C18-ARII analytical column (Nacalai Tesque, 4.6 × 250 mm, flow rate 1 mL/min) at 220 nm absorbance on a Shimadzu LC-10ADvp (Shimadzu corporation, Ltd., Kyoto, Japan). Optical rotations were measured with a JASCO P-1020 polarimeter.

4.2. Thioredoxin–polyglutamine constructs and protein purification

Thioredoxin fused to 62 glutamines (thio-Q62) were expressed in *E. coli* DH5α and purified using B-PER Bacterial Protein Extraction Reagent (Pierce Chemical, Rockford, IL) and nickel-chelating ProBond Resin columns (Invitrogen, Carlsbad, CA) as described previously.[16] The final concentration of thio-Q62 was determined by the Lowry method using a DC protein assay kit (Bio-Rad Laboratories, Hercules, CA), and its purity was examined by sodium dodecyl sulfate-polyacrylamide gel electrophoresis followed by Coomassie brilliant blue staining.

4.3. Protein aggregation turbidity assay

Aggregation of thio-Q62 protein was assessed by the turbidity assay as described previously.[16] Briefly, the thio-Q62 protein (7.5 μM) was incubated with compound in phosphate-buffered saline (PBS, pH 7.5) at 37 °C in a low-protein-binding 384-well plate, and turbidity at 405 nm was measured every 12 h using a Spectramax Plus plate reader (Molecular Devices).

4.4. CD measurement

QBP1 and peptides **12–22** were dissolved in PBS (pH 7.4) at a concentration of 10 μM. The wavelength-dependent of molar ellipticity [Q] was monitored at 20 °C as the average of eight scans in a spectropolarimeter (Model J-710; Jasco, Tokyo, Japan).

Acknowledgments

This work was supported by Grants-in-Aid for Scientific Research from the Ministry of Education, Culture, Sports, Science, and Technology of Japan. K.T. is grateful for Research Fellowships from the JSPS for Young Scientists.

Supplementary data

Supplementary data associated with this article can be found, in the online version, at doi:10.1016/j.bmc.2008.12.018.

References and notes

1. Ross, C. A.; Poirier, M. A. *Nat. Rev. Mol. Cell Biol.* **2005**, 6, 891.

2. Gusella, J. F.; MacDonald, M. E. *Nat. Rev. Neurosci.* **2000**, *1*, 109.
3. Orr, H. T.; Zoghbi, H. Y. *Annu. Rev. Neurosci.* **2007**, *30*, 575.
4. Nagai, Y.; Inui, T.; Popiel, H. A.; Fujikake, N.; Hasegawa, K.; Urade, Y.; Goto, Y.; Naiki, H.; Toda, T. *Nat. Struct. Mol. Biol.* **2007**, *14*, 332.
5. Nagai, Y.; Popiel, H. A. *Curr. Pharm. Des.* **2008**, *14*, 3267.
6. Kazantsev, A.; Walker, H. A.; Slepko, N.; Bear, J. E.; Preisinger, E.; Steffan, J. S.; Zhu, Y.-Z.; Gertler, F. B.; Housman, D. E.; Marsh, J. L.; Thompson, L. M. *Nat. Genet.* **2002**, *30*, 367.
7. Lecerf, J.-M.; Shirley, T. L.; Zhu, Q.; Kazantsev, A.; Amersdorfer, P.; Housman, D. E.; Messer, A.; Huston, J. S. *Proc. Natl. Acad. Sci. U.S.A.* **2001**, *98*, 4764.
8. Colby, D. W.; Chu, Y.; Cassady, J. P.; Duennwald, M.; Zazulak, H.; Webster, J. M.; Messer, A.; Lindquist, S.; Ingram, V. L; Wittrup, K. D. *Proc. Natl. Acad. Sci. U.S.A.* **2004**, *101*, 17616.
9. Chai, Y.; Koppenhafer, S. L.; Bonini, N. M.; Paulson, H. L. *J. Neurosci.* **1999**, *19*, 10338.
10. Cummings, C. J.; Mancini, M. A.; Antalffy, B.; DeFranco, D. B.; Orr, H. T.; Zoghbi, H. Y. *Nat. Genet.* **1998**, *19*, 148.
11. Warrick, J. M.; Chan, H. Y. E.; Gray-Board, G. L.; Chai, Y.; Paulson, H. L.; Bonini, N. M. *Nat. Genet.* **1999**, *23*, 425.
12. Heiser, V.; Scherzinger, E.; Boeddrich, A.; Nordhoff, E.; Lurz, R.; Schugardt, N.; Lehrach, H.; Wanker, E. E. *Proc. Natl. Acad. Sci. U.S.A.* **2000**, *97*, 6739.
13. Heiser, V.; Engemann, S.; Bröcker, W.; Dunkel, I.; Boeddrich, A.; Waelter, S.; Nordhoff, E.; Lurz, R.; Schugardt, N.; Rautenberg, S.; Herhaus, C.; Barnickel, G.; Böttcher, H.; Lehrach, H.; Wanker, E. E. *Proc. Natl. Acad. Sci. U.S.A.* **2002**, *99*, 16400.
14. Sánchez, I.; Mahlke, C.; Yuan, J. *Nature* **2003**, *421*, 373.
15. Tanaka, M.; Machida, Y.; Niu, S.; Ikeda, T.; Jana, N. R.; Doi, H.; Kurosawa, M.; Nekooki, M.; Nukina, N. *Nat. Med.* **2004**, *2*, 148.
16. Nagai, Y.; Tucker, T.; Ren, H.; Kenan, D. J.; Henderson, B. S.; Keene, J. D.; Strittmatter, W. J.; Burke, J. R. *J. Biol. Chem.* **2000**, *275*, 10437.
17. Takahashi, Y.; Okamono, Y.; Popiel, H. A.; Fujikake, N.; Toda, T.; Kinjo, M.; Nagai, Y. *J. Biol. Chem.* **2007**, *282*, 24039.
18. Nagai, Y.; Fujikake, N.; Ohno, K.; Higashiyama, H.; Popiel, H. A.; Rahadian, J.; Yamaguchi, M.; Strittmatter, W. J.; Burke, J. R.; Toda, T. *Hum. Mol. Genet.* **2003**, *12*, 1253.
19. Joliot, A.; Prochiantz, A. *Nat. Cell Biol.* **2004**, *6*, 189.
20. Wadia, J. S.; Dowdy, S. F. *Curr. Opin. Biotechnol.* **2002**, *13*, 52.
21. Futaki, S.; Suzuki, T.; Ohashi, W.; Yagami, T.; Tanaka, S.; Ueda, K.; Sugiura, Y. *J. Biol. Chem.* **2001**, *276*, 5836.
22. Popiel, H. A.; Nagai, Y.; Fujikake, N.; Toda, T. *Mol. Ther.* **2007**, *15*, 303.
23. Popiel, H. A.; Nagai, Y.; Fujikake, N.; Toda, T. *Neurosci. Lett.* **2009**, *449*, 87.
24. Ren, H.; Nagai, Y.; Tucker, T.; Strittmatter, W. J.; Burke, J. R. *Biochem. Biophys. Res. Commun.* **2001**, *288*, 703.
25. Yasukawa, T.; Kanei-Ishii, C.; Maekawa, T.; Fujimoto, J.; Yamamoto, T.; Ishii, S. *J. Biol. Chem.* **1995**, *270*, 25328.
26. Tyndall, J. D. A.; Pfeiffer, B.; Abbenante, G.; Fairlie, D. P. *Chem. Rev.* **2005**, *105*, 793.
27. Kaiser, E.; Colescott, R. L.; Bossinger, C. D.; Cook, P. I. *Anal. Biochem.* **1970**, *34*, 595.

ELSEVIER

Parkinsonism and Related Disorders 15, Supplement 1 (2009) S17–S20

Parkinsonism & Related Disorders

www.elsevier.com/locate/parkreldis

Levodopa in the early treatment of Parkinson's disease

Miho Murata *

Department of Neurology, National Center Hospital of Neurology & Psychiatry, Kodaira, Japan

Abstract

L-dopa has many advantages as initial therapy for Parkinson's disease (PD). It is safer, more efficacious, associated with fewer adverse effects, few interactions, easier for patients to use and for clinicians to prescribe, and cheaper than dopamine (DA) agonists. Although L-dopa is more likely than DA agonists to introduce motor fluctuations and dyskinesia, L-dopa is also more effective in improving motor function. Furthermore, there is no long-term benefit from delaying L-dopa based on the risk of motor complications or psychiatric symptoms. Many investigations have shown that L-dopa does not accelerate disease progression. Now is the time to re-evaluate L-dopa for initial treatment of PD.

Keywords: Parkinson's disease; L-dopa; DA agonist; Motor fluctuation, Dyskinesia

1. Introduction

Although it is recommended that dopamine (DA) agonists should be chosen as initial treatment for Parkinson's disease (PD), it is time to re-evaluate the use of levodopa for initial treatment of PD.

While many dopaminergic drugs have been introduced, L-dopa therapy has remained the gold standard for symptomatic treatment of PD. L-dopa is safer, more efficacious, associated with fewer adverse effects, has few interactions, is easier for patients to use and for clinicians to prescribe, and it is cheaper than DA agonists. Despite these advantages, many previous guidelines (Fig. 1) [1,2] have stated that for early stage patients with PD it is appropriate to start treatment with a DA agonist unless the patient is either older than 75 years or has dementia. The rationale for these recommendations has been that (1) L-dopa may accelerate disease progression, and (2) DA agonists are less likely to induce motor fluctuation.

2. Is L-dopa really neurotoxic?

Concern that exogenous L-dopa may be neurotoxic and contribute to the progression of PD arises from the oxidative stress hypothesis of PD [3]. Many *in vitro* studies have demonstrated that the addition of L-dopa or DA to cultured dopaminergic neurons increased cell death [4,5]. However, these experiments were performed under non-physiologic conditions; the concentrations of L-dopa and DA in these experiments were high (>5 μM) and exceeded what would be expected in the brains of patients treated with therapeutic doses (<2 μM). Furthermore, some *in vitro* studies have shown that L-dopa and DA are neuroprotective when neurons are co-cultured with glial cells [6,7].

The ELLDOPA study, conducted to show whether L-dopa is toxic for PD patients, was a large, double-blind, randomized, controlled clinical trial comparing three different doses (150, 300, 600 mg per day) of L-dopa with placebo in patients with early PD [8]. At the end of the trial (after a 2-week washout period), the mean Unified Parkinson's Disease Rating Scale (UPDRS) score of patients treated with L-dopa was better than that of the placebo group. The mean UPDRS score of the highest dosage group was the best, even after the washout period. These results suggest that L-dopa is not toxic, and may even be neuroprotective. This study also included evaluation with β-CIT SPECT

* Address for correspondence: Miho Murata, MD, PhD. National Center Hospital of Neurology & Psychiatry, 4-1-1 Ogawahigashi, Kodaira, Tokyo, Japan 187-8551. Tel.: 81-42-341-2711; Fax: 81-42-346-1735.
E-mail address: mihom@ncnp.go.jp

1353-8020/$ – see front matter

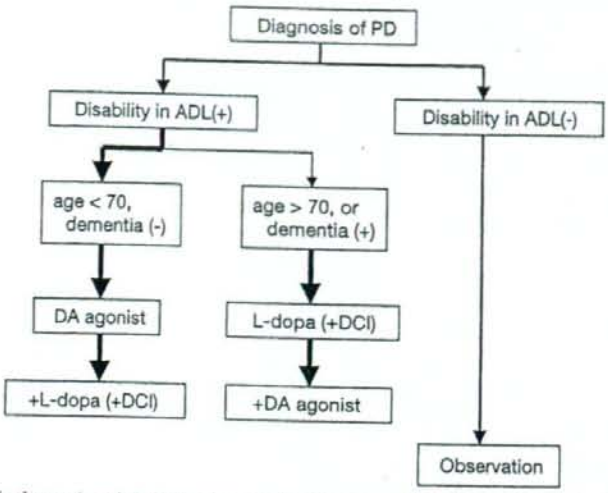

Fig. 1. Guideline for Parkinson's disease (early stage) made by Japanese Society for Neurology, 2002. ADL, activities of daily living; DCI, decarboxylase inhibitor.

imaging, as a marker for intact nigrostriatal dopaminergic neuronal functioning. The imaging studies showed that there was a larger decrease in β-CIT uptake in patients treated with L-dopa in a dose–response manner. These clinical and imaging results suggested that β-CIT SPECT imaging is not appropriate for evaluating the neuroprotective ability of the drugs. Up to that time, several studies had shown that DA agonists are more protective than L-dopa using β-CIT SPECT [9,10] or F-DOPA PET [11]. The results of the ELLDOPA study permitted re-evaluation of the results of these studies, and there is now a consensus that L-dopa does not accelerate disease progression [12].

3. L-dopa is more likely than DA agonists to induce motor fluctuations and dyskinesia

Several clinical studies [9,11] have shown that treatment with DA agonists is less likely to induce motor complications than treatment with L-dopa. Theses studies also showed that L-dopa monotherapy improves activities of daily living and motor function to a greater degree than DA agonists (plus later optional L-dopa). What is of most importance to our patients? The severity of both motor fluctuation and dyskinesia in these studies was low. For example, in the CALM-PD study (4 years) the percentage of disabling dyskinesia was 4.4% in the pramipexole group and 6.9% in the L-dopa group [13]. Furthermore, retrospective investigations failed to show any long-term benefit from delaying L-dopa based on the risk of motor complications, dementia, or psychiatric symptoms [13–16].

Apart from motor complications, the frequency of other common side effects is less with L-dopa than with DA agonists. For example, hallucinations are about three times more likely to occur with ropinirole or pramipexole than with L-dopa [17]. Somnolence, edema, and cardiac valvular fibrosis (pergolide, cabergoline) are also more frequent with DA agonist treatment than with L-dopa [17]. In Japan, those who are taking ropinirole or pramipexole are prohibited from driving because of the risk of sudden onset sleep. Can the incidence of motor fluctuation be reduced only at the expense of improvements in motor function and activities of daily living, and of other side effects such as hallucination, sudden onset sleep, and fibrosis?

4. Mechanism of wearing-off

Disease progression is associated with "wearing off" of therapeutic benefit and the appearance of unpredictable treatment responses, resulting in complex "on-off" response fluctuations. These arise in between doses of L-dopa because the patient no longer has the ability to store dopamine. The other factors driving development of response fluctuations are changes in peripheral L-dopa pharmacokinetics and in post-synaptic function that accompany large-dose and long-term L-dopa therapy [18]. Jenner and colleagues reported on the relation between the amount of lesion and the development of dyskinesia and motor fluctuation by using a 1-methyl-4-phenyl-1,2,3,6-tetrahydropyridine (MPTP) marmoset model [19]. In primates with 50% lesions (model of early PD), L-dopa produced an antiparkinsonian response with no induction of dyskinesia. In the group with 75% lesions, L-dopa produced an antiparkinsonian response with a gradual development of dyskinesia. In the >90% lesion group, L-dopa produced a pulsatile anitiparkinsonian response and rapid induction of severe dyskinesia.

Pathological examination in patients with PD demonstrates an exponential loss of nigral pigmented neurons [20]. At 5 years from symptom onset, about 50% of the pigmented neurons remain, compared with age-adjusted controls, and at 10 years 30% remain. The presymptomatic phase of PD, dating from the onset of neuronal loss, was estimated to be about 5 years. Therefore, at the initial symptomatic stage

of the disease there is little possibility of developing motor fluctuation and dyskinesia as long as the appropriate dose of L-dopa is used. In fact, the ELLDOPA study showed the incidence of motor complications in the L-dopa 150 mg and 300 mg groups to be almost equal to that in the placebo group [8].

5. The advantage of L-dopa as initial therapy for Parkinson's disease

The initial use of L-dopa for the symptomatic treatment of PD has many advantages over DA agonists: (1) L-dopa has significantly greater efficacy than DA agonists in alleviating the motor symptoms of PD and improving activities of daily living. (2) Titration of L-dopa to therapeutic levels is much easier and faster than that of DA agonists. (3) L-dopa is much less likely to induce hallucinations, somnolence, edema, or constipation compared to DA agonists. (4) There is a clear cost benefit to using L-dopa. (In Japan, L-dopa + decarboxylase inhibitor 300 mg/day costs about 1 US dollar per day; pramipexole 4.5 mg/day about 16 US dollars; and ropinirole 15 mg/day 26 US dollars.) However, late-developing motor fluctuation and dyskinesia deserve consideration, and the potential for other common side effects such as hallucinations and sleep attacks must also be factored into the treatment decision. Furthermore, early in the course of the disease, L-dopa provides an enduring response that can last several days [21].

There is much evidence to show that DA agonists are efficacious in controlling L-dopa motor fluctuations (as later adjunctive therapy). However, another option is to initiate treatment with levodopa, adding a DA agonist after the first sign of developing motor complications has appeared (early combination).

6. Continuous stimulation by using L-dopa

Continuous daytime intraintestinal infusion of L-dopa can diminish motor complications [22]. This shows that motor complications can be improved by changing the pharmacokinetics of L-dopa. For example, catechol-*O*-methyltransferase (COMT) inhibitors can extend the half-life of serum L-dopa concentration. The duration of L-dopa efficacy can also be extended by taking L-dopa after a meal (Fig. 2). Long-term L-dopa therapy increases the peak L-dopa concentration (C_{max}) and decreases its half-life ($T_{1/2}$) [23]. C_{max} is decreased and $T_{1/2}$ is increased by taking L-dopa after a meal compared to taking it before meals. Therefore, taking L-dopa after meals not only extends effective time but also decreases dyskinesia. By taking L-dopa after meals, the dose of L-dopa can be increased, but the risk of dyskinesia can be decreased. If needed, a low dose of L-dopa may be taken before meals for immediate improvements, with the remainder of the dose taken after meals.

There is much evidence for the efficacy of DA agonists as adjunctive therapy in controlling L-dopa motor fluctuations and dyskinesia [24]. Monoamine oxidase (MAO) B inhibitors [24] and zonisamide [25] may also be used as adjunctive therapy to improve motor fluctuations.

7. Initial symptomatic treatment for early Parkinson's disease

It is appropriate to start treatment of PD with either L-dopa or DA agonists. As highlighted by the American Academy of Neurology practice parameter [17], the choice of initial treatment depends on the relative importance for the patient of improving motor disability and limiting adverse events versus the possibility of lowering the risk of developing long-term motor complications.

The frequency of the development of wearing-off depends on the age of disease onset. Younger-onset patients (younger than 50 years at onset) are more prone to severe dyskinesia and motor fluctuation, while patients older than 70 years at symptom-onset rarely develop disabling dyskinesia and motor fluctuation. Older patients may be more prone to develop hallucinations and other common adverse effects. Therefore, L-dopa is preferred for elderly patients as initial treatment. In younger patients, DA agonists are preferred, but if the patient is at risk of losing his or her job owing to motor disability, L-dopa should be started. Patients whose age of onset is between 50 and 70 years can be prescribed

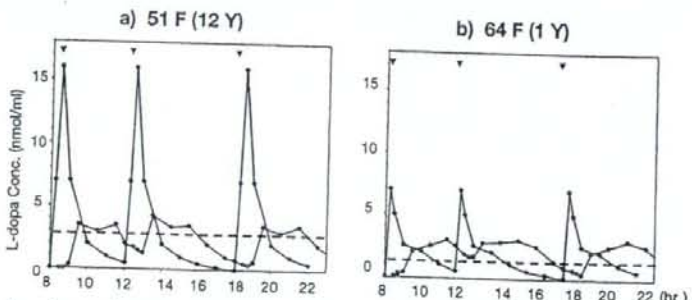

Fig. 2. Effects of a meal on L-dopa pharmacokinetics. (a) 51-year-old woman with 12 years' duration of Parkinson's disease. (b) 64-year-old woman with 1 year duration of Parkinson's disease. A tablet of L-dopa 100 mg + benserazide 20 mg was taken. Black curve: just before meal, red curve: after meal 3 times a day. ▼: meals (at 08.00, 12.00, 18.00 hours). Dashed line: the concentration of effective threshold estimated by clinical symptoms. C_{max} is 2–3 times higher when L-dopa was taken before meals than after meals. L-dopa pharmacokinetics are more stable when taken after meals than before meals.

either L-dopa or a DA agonist. Treatment selection should reflect the patient's needs and under-treatment should be avoided.

Conflict of interest

The author has no conflict of interest to report. No funding applicable.

References

[1] Olanow CW, Koller WC. An algorithm (decision tree) for the management of Parkinson's disease: treatment guidelines. American Academy of Neurology. Neurology 1998;50(Suppl 3):S1–57.

[2] Mizuno Y, Okuma Y, Kikuchi S, Kuno S, Hashimoto T, Hasegawa K, et al. Guidelines for the treatment of Parkinson's disease. Clin Neurol 2002;42:430–94.

[3] Fahn S. Is levodopa toxic? Neurology 1996;47(Suppl 3):S184–95.

[4] Pardo B, Mena MA, Casarejos MJ, Paino CL, De Yebenes JG. Toxic effects of L-DOPA on mesencephalic cell cultures: protection with antioxidants. Brain Res 1995;682:133–43.

[5] Masserano JM, Gong L, Kulaga H, Baker I, Wyatt RJ. Dopamine induces apoptotic cell death of a catecholaminergic cell line derived from the central nervous system. Mol Pharmacol 1996;50:1309–15.

[6] Mena MA, Casarejos MJ, Carazo A, Paino CL, Garcia de Yebenes J. Glia conditioned medium protects fetal rat midbrain neurons in culture from L-DOPA toxicity. Neuroreport 1996;76:441–5.

[7] Mytilineou C, Han SK, Cohen G. Toxic and protective effects of L-dopa on mesencephalic cell cultures. J Neurochem 1993;61:1470–8.

[8] The Parkinson Study Group. Levodopa and the progression of Parkinson's disease. New Engl J Med 2004;351:2498–508.

[9] Parkinson Study Group. Pramipexole vs levodopa as initial treatment for parkinson disease. JAMA 2000;284:1931–8.

[10] Parkinson Study Group. Dopamine transporter brain imaging to assess the effects of pramipexole vs levodopa on Parkinson disease progression. JAMA. 2002;287:1653–61.

[11] Whone AL, Watts RL, Stoessl AJ, Davis M, Reske S, Nahmias C, et al. Slower progression of Parkinson's disease with ropinirole versus levodopa: The REAL-PET study. Ann Neurol 2003;54:93–101.

[12] Suchowersky O, Gronseth G, Perlmutter J, Reich S, Zesiewicz T, Weiner WJ, et al. Practice Parameter: Neuroprotective strategies and alternative therapies for Parkinson disease (an evidence-based review). Neurology 2006;66:976–82.

[13] Halloway RG, Shoulson I, Fahn S, Kiburtz K, Lang A, Marek K, et al. Pramipexole vs levodopa as initial treatment for Parkinson disease: a 4-year randomized controlled trial. Arch Neurol 2004;61:1044–53.

[14] Caracenti T, Scigliano G, Musicco M. The occurrence of motor fluctuations in Parkinsonian patients treated long-term with levodopa: role of early treatment and disease progression. Neurology 1991;41:380–4.

[15] Cedarbaum JM, Gandy SE, McDowell FH. Early initiation of levodopa treatment of motor response fluctuations, dyskinesia or dementia in Parkinson's disease. Neurology 1991;41:622–9.

[16] Lees AJ, Katzenschlager R, Head J, Ben-Shlomo Y. Ten-year follow-up of these different initial treatments in de-novo PD. A randomized trial. Neurology 2001;51:1687–94.

[17] Miyasaki JM, Martin W, Suchowsky O, Weiner WJ, Lang AE. Practice parameter: Initiation of treatment for Parkinson's disease: An evidence-based review. Neurology 2002;58:11–7.

[18] Poewe W, Wenning G. Levodopa in Parkinson's disease: mechanisms of action and pathophysiology of late failure. In: Jankovic JJ, Tolosa E, editors. Parkinson's Disease & Movement Disorders, 4th ed. Philadelphia: Lippincott Williams & Wilkins; 2002. p. 104–15.

[19] Jenner P, Jackson M, Rose S, Smith L. Co-administration of LDOPA/carbidopa with entacapone avoids dyskinesia induction in MPTP-treated primates with full or partial nigral lesions. Mov Disord 2006;(suppl 13):S73.

[20] Fearnley JM, Lees AJ. Ageing and Parkinson's disease: Substantia nigra regional selectivity. Brain 1991;114:2283–301.

[21] Muenter MD, Tyce GM. L-dopa therapy of PD in plasma L-DOPA concentration, therapeutic response, and side effects. Mayo Clin Proc 1971;46:231–9.

[22] Stocchi F, Vacca L, Ruggieri S, Olanow CW. Intermittent vs continuous levodopa administration in patients with advanced Parkinson disease. Arch Neurol 2005;62:905–10.

[23] Murata M, Mizusawa H, Yamanouchi H, Kanazawa I. Chronic levodopa therapy enhances dopa absorption: contribution to wearing-off. J Neural Transm 1996;103:1177–85.

[24] Pahwa R, Factor SA, Lyons KE, Ondo WG, Gronseth G, Bronte-Stewart H, et al. Practice parameter: Treatment of Parkinson disease with motor fluctuations and dyskinesia (an evidence-based review). Neurology 2006;66:983–95.

[25] Murata M, Hasegawa K, Kanazawa I. Zonisamide improves motor function in Parkinson's disease. A randomized, double-blind study. Neurology 2007;68:45–50.

Available online at www.sciencedirect.com
ScienceDirect
Neuroscience Research 60 (2008) 106–113
Neuroscience Research
www.elsevier.com/locate/neures

Preventing effects of a novel anti-parkinsonian agent zonisamide on dopamine quinone formation

Masato Asanuma [a,*], Ikuko Miyazaki [a], Francisco J. Diaz-Corrales [a], Ko Miyoshi [a], Norio Ogawa [a], Miho Murata [b]

[a] *Department of Brain Science, Okayama University Graduate School of Medicine, Dentistry and Pharmaceutical Sciences, 2-5-1 Shikatacho, Okayama 700-8558, Japan*
[b] *Department of Neurology, Musashi Hospital, National Center of Neurology and Psychiatry, Tokyo, Japan*

Received 10 August 2007; accepted 3 October 2007
Available online 10 October 2007

Abstract

The neurotoxicity of dopamine (DA) quinones as dopaminergic neuron-specific oxidative stress is considered to play a role in the pathogenesis and/or progression of Parkinson's disease (PD), since DA quinones conjugate with several key PD pathogenic molecules (*e.g.*, tyrosine hydroxylase, α-synuclein and parkin) to form protein-bound quinone (quinoprotein) and consequently inhibit their functions. Zonisamide (ZNS) is used as an anti-epileptic agent but also improved the cardinal symptoms of PD in recent clinical trials in Japan. To evaluate the effects of ZNS on excess cytosolic free DA-induced quinone toxicity, we examined changes in DA quinone-related indices after ZNS treatment both in *in vitro* cell-free system and in cultured cells. Co-incubation of DA and ZNS in a cell-free system caused conversion of DA to stable melanin via formation of DA-semiquinone radicals and DA chrome. Long-term (5 days) treatment with ZNS decreased quinoprotein and increased DA/DOPA chromes in dopaminergic CATH.a cells. ZNS significantly inhibited quinoprotein formation induced by treatment with tetrahydrobiopterin and ketanserin that elevate cytosolic free DA in the cells. Our results suggest that the novel anti-parkinsonian agent ZNS possesses preventing effects against DA quinone formation induced by excess amount of cytosolic DA outside the synaptic vesicles.

Keywords: Zonisamide; Dopamine chrome; Dopamine quinone; Quinoprotein; Parkinson's disease

1. Introduction

Under normal conditions, dopamine (DA) is stable in the synaptic vesicle. However, when levodopa is administered to the damaged dopaminergic neuronal system of Parkinson's disease (PD), a large amount of DA remains in the cytosol outside the synaptic vesicle, since the damaged dopaminergic system has too small DA pool to store DA (Sulzer et al., 2000; Sulzer and Zecca, 2000; Asanuma et al., 2003; Ogawa et al., 2005). The toxicity of excess levodopa and/or DA has been well documented in many *in vitro* and *in vivo* animal studies using parkinsonian models (Ogawa et al., 1993; Basma et al., 1995; Walkinshaw and Waters, 1995; Hastings et al., 1996; Asanuma et al., 2003), despite its marked beneficial effects.

Free excess DA is easily metabolized via monoamine oxidase (MAO)-B or by auto-oxidation to produce cytotoxic reactive oxygen species (ROS), and then forms neuromelanin (Sulzer et al., 2000; Sulzer and Zecca, 2000). In the oxidation of DA by MAO, DA is converted to dihydroxyphenylacetic acid (DOPAC) to generate general ROS hydrogen peroxide. On the other hand, non-enzymatic and spontaneous auto-oxidation of DA and L-DOPA produces superoxide and reactive quinones such as DA quinones and DOPA quinones (Tse et al., 1976; Graham, 1978). DA quinones are also generated in the enzymatic oxidation of DA by prostaglandin H synthase (cyclooxygenase-2), lipoxygenase, tyrosinase and xanthine oxidase (Korytowski et al., 1987; Rosei et al., 1994; Hastings, 1995; Foppoli et al., 1997; Chae et al., 2007). These quinones are oxidized to the cyclized aminochromes: DA chrome (aminochrome) and DOPA chrome, and then are finally polymerized to form melanin. Although ROS generation by the auto-oxidation of DA may explain widespread

* Corresponding author. Tel.: +81 86 235 7408; fax: +81 86 235 7412.
E-mail address: asachan@cc.okayama-u.ac.jp (M. Asanuma).

0168-0102/$ – see front matter
doi:10.1016/j.neures.2007.10.002

toxicity but not specific damage of DA neurons, the highly reactive DA quinone or DOPA quinone itself exerts predominant cytotoxicity in DA neurons and surrounding neural cells, since these quinones are generated from free cytosolic DA outside the synaptic vesicle or from L-DOPA (Sulzer et al., 2000).

The generated DA quinones covalently conjugate with the sulfhydryl group of cysteine on functional proteins, resulting predominantly in the formation of 5-cysteinyl-DA (Graham, 1978; Fornstedt et al., 1986). DA quinones conjugate with cysteine residues of various functional proteins including several key molecules involved in the pathogenesis of PD (*e.g.*, tyrosine hydroxylase, DA transporter and parkin) to form protein-bound quinones (quinoproteins), and inhibit the function of these proteins to cause DA neuron-specific cytotoxicity (Xu et al., 1998; Kuhn et al., 1999; Whitehead et al., 2001; LaVoie et al., 2005; Machida et al., 2005). We reported previously that repeated levodopa administration elevated striatal DA turnover and formation of quinoproteins specifically in the parkinsonian side, but not in the control side, of hemi-parkinsonian models (Ogawa et al., 2000; Asanuma et al., 2005; Miyazaki et al., 2005). Therefore, the excess amount of cytosolic DA outside the synaptic vesicles after levodopa treatment may exert neurodegenerative effects through quinone generation, at least in the damaged dopaminergic nerve terminals. The DA-induced formation of DA quinones and the consequent dopaminergic cell damage *in vitro* and *in vivo* could be prevented by treatment with superoxide dismutase, glutathione, and certain thiol reagents through their quinone-quenching activities (Offen et al., 1996; Lai and Yu, 1997; Kuhn et al., 1999; Haque et al., 2003). We also demonstrated recently that DA agonists pergolide and pramipexole exhibit quenching properties against *in vitro* generated DA-semiquinone radicals (Asanuma et al., 2005; Miyazaki et al., 2005), and that pergolide effectively prevented repeated levodopa-induced elevation of striatal quinoprotein specifically in parkinsonian models (Miyazaki et al., 2005). Thus, DA quinones act as neurotoxic compounds by eliciting dopaminergic neuron-specific oxidative stress and thus play a role in the pathogenesis and/or progression of PD and neurotoxin-induced parkinsonism (Choi et al., 2003, 2005; Asanuma et al., 2004; LaVoie et al., 2005; Machida et al., 2005; Ogawa et al., 2005; Chae et al., 2007).

Zonisamide (1,2-benzisoxazole-3-methaesulfonamide: ZNS), which was originally synthesized in Japan, has been used as an anti-epileptic agent in Japan, South Korea, USA and Europe. An open trial of ZNS (50–200 mg/day) administered in conjunction with anti-PD drugs showed lessening of symptoms, especially wearing-off (Murata et al., 2001), and induced more than 30% improvement of UPDRS total score up to 3 years (Murata, 2004). The addition of ZNS to levodopa treatment of patients experiencing 'wearing-off' fluctuations resulted in lessening of motor fluctuation and significant improvement of the duration, severity and activities of daily living in 'off' time and score of motor examination. Furthermore, a recent nationwide double-blind controlled study in Japan reported that an adjunctive treatment with lower dose of ZNS (25–100 mg/day) to levodopa improved all the cardinal symptoms of PD (Murata, 2004; Murata et al., 2007).

Several pharmacological effects of ZNS have been proposed to be related to its beneficial effects on PD. ZNS is a specific T-type Ca^{++} channel blocker (Suzuki et al., 1992; Kito et al., 1996), which increases burst firing of dopaminergic neurons in the substantia nigra. A single dose of ZNS increased intracellular and extracellular DOPA, DA and homovanillic acid (HVA) levels and decreased DOPAC level in the rat striatum presumably through its moderate MAO-inhibiting effect (Okada et al., 1992, 1995). Long-term administration of ZNS increased activity and protein level of tyrosine hydroxylase in the rat striatum (Murata, 2004), and thus enhanced DA synthesis. However, these effects cannot fully explain the mechanism of its therapeutic effects on levodopa-induced adverse effects.

To evaluate the effects of ZNS on excess cytosolic free DA-induced quinone toxicity, we examined changes in DA quinone-related indices after ZNS treatment both in *in vitro* cell-free DA-semiquinone generating system and in cultured dopaminergic neuronal cells.

2. Materials and methods

2.1. Materials

DA hydrochloride and L-DOPA were purchased from Wako Pure Chemical (Tokyo, Japan) and Sigma (St. Louis, MO), respectively. ZNS and its sodium salt were provided by Dainippon Sumitomo Pharma (Osaka, Japan).

2.2. ESR spectrometry of generated DA-semiquinone radicals

The spectra of semiquinone radicals generated from DA in a cell-free system were recorded with an electron spin resonance (ESR) spectrometer (JES-FR30, JEOL Co., Tokyo) using a flat quartz cuvette as reported previously (Korytowski et al., 1987; Haque et al., 2003). DA or L-DOPA was dissolved in 10 mM sodium phosphate buffer (PB: pH 7.4), and the pH was adjusted to 7.0 by adding 0.1 M NaOH at 4 °C. For the experiment on time-dependency, the pH-adjusted DA or L-DOPA (final concentration 1 mM) was immediately incubated with ZNS sodium salt dissolved in 10 mM PB (final concentration 8 mM, pH 10.8) for 1–60 min at 37 °C, and the spectra for these combinations were analyzed. As a positive control to generate DA-semiquinone, tyrosinase (final concentration 12.5 μg/ml) was incubated instead of ZNS. Furthermore, 0.1 N NaOH (pH 10.9) or pH-adjusted 10 mM PB (pH 10.8) was used instead of ZNS as a negative control. For the experiment on dose-dependency, the pH-adjusted DA (final concentration 1 mM, pH 7.0), with or without various concentrations (ranging from 2 to 8 mM) of ZNS sodium salt dissolved in 10 mM PB (pH 10.8), was immediately incubated for 1 min at 37 °C, and the spectra for these combinations were analyzed. The pH of each final incubation mixture was approximately 8.0. The signal intensity was evaluated by the relative peak height of the second signal of the semiquinone radical spin adduct (the peak height of the second signal is higher than the others and is directly proportional to double integration of the spectra) to the intensity of the Mn^{2+} signal, which was used as the internal standard to correct for measurement error. The conditions of the ESR spectrometer to estimate the semiquinone radical, including magnetic field, power, modulation frequency, modulation amplitude, response time, temperature, amplitude, and sweep time were 335 ± 5 mT, 4 mW, 9.41 GHz, 79 μT, 0.1 s, 25 °C, 1 × 1000 and 1 min, respectively. Furthermore, the levels of DA and its metabolites in the reaction mixture were measured by high-performance liquid chromatography (HPLC) as described previously (Ogawa et al., 2000; Asanuma et al., 2005).

2.3. Effects of ZNS on generation of DA chrome

To examine the effects of ZNS on generation of DA chrome in a cell-free system, pH-adjusted 1 mM DA in 10 mM PB (pH 6.8) and 0.2% Triton X-100 solution were incubated with or without 200 μM ZNS dissolved in 10 mM PB (pH 6.8) for 1 min to 3 h at 37 °C. The level of DA chrome in the final mixture (pH 6.8) was estimated by measuring absorbance of incubation mixture at 475 nm.

2.4. Cell culture and drug treatment

Dopaminergic CATH.a cells (ATCC; #CRL-11179), derived from mouse DA-containing neurons, were cultured at 37 °C in 5% CO_2 in RPMI 1640 culture medium (Invitrogen, San Diego, CA) supplemented with 4% fetal bovine serum, 8% horse serum, 100 U/ml penicillin and 100 μg/ml streptomycin. Cells were seeded in 6-well plates (Becton Dickinson Labware, Franklin Lakes, NJ) for the extraction of cell lysates used for the measurement of protein-bound quinone and DA/DOPA chrome at a density of 1.0×10^5 cells/cm^2. After 24 h, CATH.a cells were exposed to 1–100 μM ZNS diluted in phosphate buffered saline (PBS) for 5 days for the measurements of quinoprotein and DA/DOPA chrome. To examine the effects of ZNS on excess cytosolic free DA-induced quinone elevation, CATH.a cells were exposed simultaneously to 1–100 μM ZNS with 100 μM tetrahydrobiopterin (BH_4) and 10 μM ketanserin, which enhance DA synthesis and blocks vesicle monoamine transporter, respectively (Choi et al., 2005), for 3 h before extraction of total cell lysates for quinoprotein measurement.

2.5. Protein-bound quinone; quinoprotein measurement

Total cell lysates from drug-treated CATH.a cells were prepared with 10 μg/ml phenylmethylsulfonyl fluoride (Sigma) in ice cold-RIPA buffer [PBS (pH 7.4), 1% nonidet P-40 (NP-40), 0.5% sodium deoxycholate and 0.1% sodium dodecyl sulfate]. The nitrobluetetrazolium (NBT)/glycinate colorimetric assay was performed to detect protein-bound quinones (quinoprotein) (Paz et al., 1991). The cell lysate was added to 500 μl of NBT reagent (0.24 mM NBT in 2 M potassium glycinate, pH 10.0) followed by incubation in the dark for 2 h under constant shaking. The absorbance of blue-purple color developed in the reaction mixture was measured at 530 nm.

2.6. Measurement of DA/DOPA chrome in CATH.a cells

For the measurement of DA/DOPA chrome, cells were solubilized in 500 μl of 1% Triton X-100 solution for 2 h and then centrifuged at 20,000 × *g* for 30 min at 4 °C. The supernatant was used as cell extract and incubated for 3 min at room temperature. The level of DA/DOPA chrome was calculated by measuring absorbance of incubated cell extract at 475 nm. Absorbance values in the *in vitro* incubation of DA (0–500 μM) with tyrosinase (10 μg/ml) for 30 min were used as a standard to calculate the concentration of DA/DOPA chrome in the cell extract.

2.7. Protein measurement

The protein concentration was determined using the Bio-Rad protein assay kit or Bio-Rad DC protein assay kit (Bio-Rad, Richmond, CA), based on the method of Bradford and Lowry, respectively, using bovine serum albumin as a standard.

2.8. Statistical analysis

Results are expressed as mean ± S.E.M. values. Statistical analysis of the data was performed using one-way ANOVA followed by *post hoc* Fisher's PLSD test. A *p*-value less than 0.05 denoted the presence of a statistically significant difference.

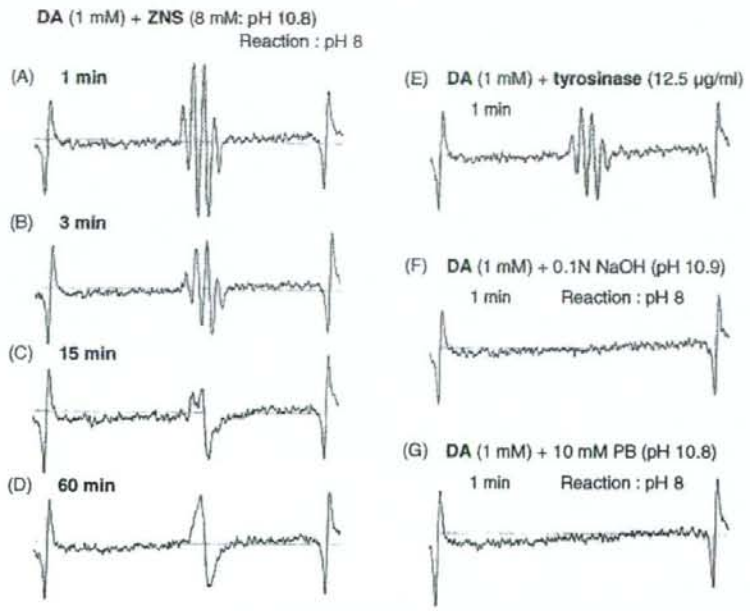

Fig. 1. Effects of ZNS on DA-semiquinone radicals generated from DA in a cell-free system. (A–D) Representative time-course changes in ESR spectra of DA-semiquinone radicals (A–B) to melanin (D) in the incubation of pH-adjusted 1 mM DA (pH 7.0) with 8 mM ZNS (sodium salt) in 10 mM PB (pH 10.8) for 1–60 min at 37 °C at pH 8.0 (incubation mixture). (E) Formation of DA-semiquinone radicals via tyrosinase (12.5 μg/ml)-catalyzed oxidation of 1 mM DA. (F and G) No signals for radical formation at pH 8.0 (incubation mixture) when pH-adjusted 1 mM DA (pH 7.0) was incubated for 1 min at 37 °C with 0.1 N NaOH (pH 10.9) (F) or pH-adjusted 10 mM PB (pH 10.8) (G). Each experiment was performed as triplicate assays.

3. Results

3.1. Effects of ZNS on generated DA-semiquinone radicals in a cell-free system

When a high dose of DA (5 mM) was incubated at 37 °C at neutral pH 7–8, the formation of DA-semiquinone radicals started immediately within 1 min, peaked at around 1 min, then gradually decreased and continued for 10 min, as shown in a previous study (Haque et al., 2003). In the present ESR study, however, no signals for radical formation were detected at pH 8 (incubation mixture) when a lower dose of pH-adjusted 1 mM DA (pH 7.0) was incubated for 1 min at 37 °C with 0.1 N NaOH (pH 10.9) or pH-adjusted 10 mM PB (pH 10.8) (Fig. 1F and G). Interestingly, when pH-adjusted 1 mM DA (pH 7.0) was incubated at 37 °C with 8 mM ZNS (sodium salt) in 10 mM PB (pH 10.8), the formation of DA-semiquinone radicals, which was identified by four waves in ESR spectrometry, started immediately within 1 min and peaked at around 1 min, at pH 8 (incubation mixture) (Fig. 1A and B), as well as formation of DA-semiquinone radicals via tyrosinase-catalyzed oxidation of DA (Fig. 1E). Then, the DA-semiquinone radical induced by incubation of DA and ZNS converted to melanin, which was recognized by a wide single wave, at 15–60 min (Fig. 1C and D). The incubation of pH-adjusted 1 mM DA (pH 7.0) and 2–8 mM ZNS (sodium salt, pH 10.8) at pH 8 (incubation mixture) resulted in DA-semiquinone radical formation at 1 min (Fig. 2A–D) and subsequent melanin formation at 60 min (data not shown) in a ZNS concentration-dependent manner. Furthermore, incubation of pH-adjusted 1 mM L-DOPA (pH 7.0) with 8 mM ZNS (sodium salt, pH 10.8) at 37 °C at pH 8 (incubation mixture) resulted in immediate generation of DOPA-semiquinone radicals within 1 min, with a peak at around 1 min, and conversion to melanin within up to 20 min (Fig. 2E–G). DOPAC, 3-methoxy tyramine and HVA, which are metabolites of DA via MAO and/or catecholamine *o*-methyltransferase, were not detected in any incubation mixture of pH-adjusted DA and ZNS (sodium salt) at either dose of ZNS or incubation time by HPLC (data not shown).

3.2. Effects of ZNS on generation of DA chrome in a cell-free system

Because a high dose of ZNS was required to detect the conversion effects from DA to melanin in ESR spectrometry, we used sodium salt of ZNS, which is highly soluble in 10 mM PB, at a dose of 2–8 mM. However, the pH value of the mixture of ESR examination was slightly alkaline at 8.0 because of high alkalinity of ZNS sodium salt solution (pH 10.8) in the cell-free system. To examine the effects of relatively low dose of ZNS on conversion of DA to melanin at neutral pH, we evaluated generation of DA chrome, which is an intermediate in conversion of DA quinone to melanin, using 200 μM ZNS at pH 6.8, but not its sodium salt (Fig. 3). Although the incubation of pH-adjusted 1 mM DA (pH 6.8) alone at 37 °C showed time-dependent but not significant increases in DA

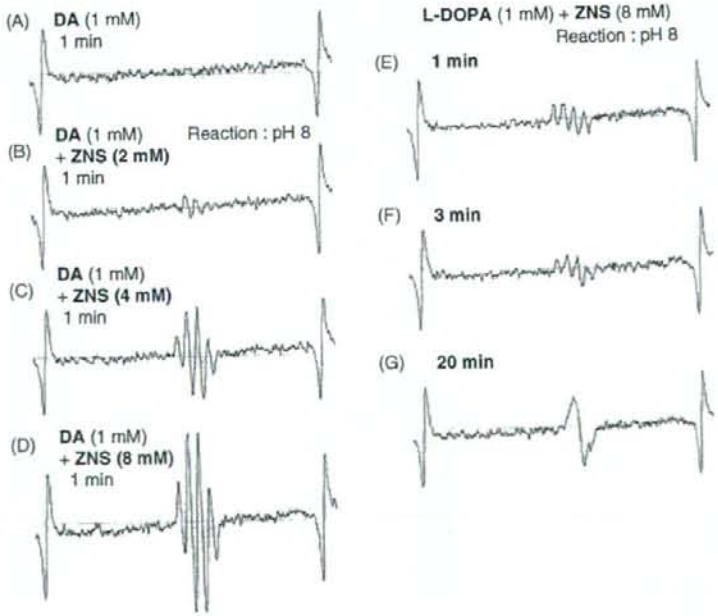

Fig. 2. Effects of ZNS on semiquinone radicals generated from DA or L-DOPA. (A–D) Dose-dependent effects of ZNS on DA-semiquinone radicals generated from DA in a cell-free system. The pH-adjusted 1 mM DA (pH 7.0) was simultaneously incubated with 2–8 mM ZNS (pH 10.8) at pH 8.0 (incubation mixture) for 1 min at 37 °C, and then the relative signal intensity of DA-semiquinone radicals was measured by ESR spectrometry. (E–G) Representative time-course changes in ESR spectra of DOPA-semiquinone radicals (E and F) to melanin (G) in the incubation of pH-adjusted L-DOPA (1 mM, pH 7.0) with 8 mM ZNS (sodium salt) in 10 mM PB (pH 10.8) for 1–20 min at 37 °C at pH 8.0 (incubation mixture). Three independent assays were performed in each experiment.

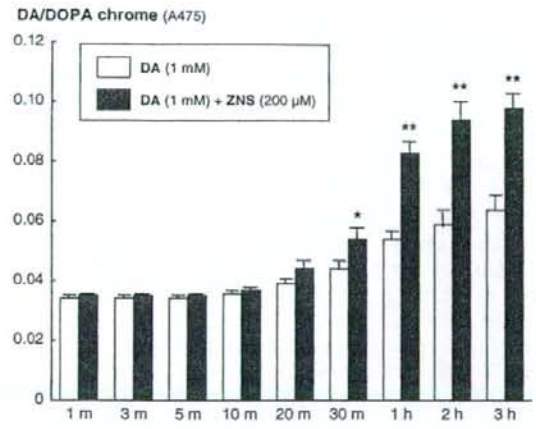

Fig. 3. Effects of ZNS on time-course changes in DA/DOPA chrome generated in a cell-free system. Levels of generated DA/DOPA chrome were measured after incubation of pH-adjusted 1 mM DA (pH 6.8) with/without 200 μM ZNS (pH 6.8) at 37 °C for 1 min to 3 h. Co-incubation of pH-adjusted DA (1 mM) and ZNS (200 μM) at neutral pH significantly increased DA/DOPA chrome at 30 min to 3 h, compared with time-matched pH-adjusted DA alone. Each value is the mean of absorbance at 475 nm ± S.E.M. ($n = 5$). $^{*}p < 0.05$, $^{**}p < 0.001$ compared with time-matched group treated with DA alone.

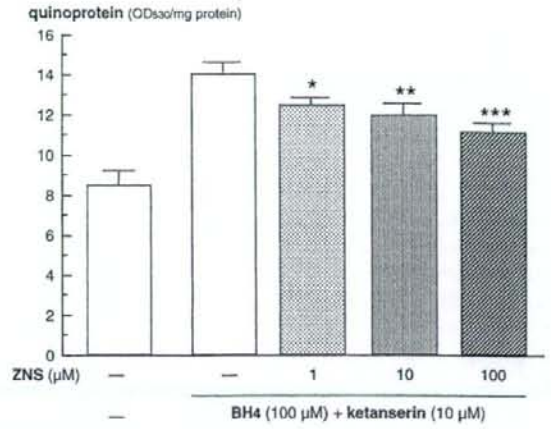

Fig. 5. Effects of ZNS treatment on excess cytosolic free DA-induced quinoprotein formation in dopaminergic CATH.a cells. Quinoprotein level in CATH.a cells were measured after treatment with BH_4 (100 μM) and ketanserin (10 μM), with or without ZNS (1–100 μM) for 3 h. The simultaneous treatment of ZNS (1–100 μM) significantly and dose-dependently inhibited BH_4 plus ketanserin-induced quinoprotein formation. Data are mean ± S.E.M. ($n = 8$). $^{*}p < 0.05$, $^{**}p < 0.01$ and $^{***}p < 0.001$ compared with cells treated with BH_4 plus ketanserin without ZNS.

chrome level, co-incubation of pH-adjusted 1 mM DA (pH 6.8) and 200 μM ZNS (pH 6.8) at 37 °C significantly increased DA chrome at 30 min to 3 h, compared with time-matched pH-adjusted DA alone.

3.3. Effects of ZNS on DA quinone formation in CATH.a cells

We examined changes in DA, its metabolites, quinoprotein and DA/DOPA chrome using *in vitro* dopaminergic CATH.a cells after 5-day treatment of ZNS. Quinoprotein level was significantly decreased after 5-day treatment of ZNS (10–100 μM) (Fig. 4) with reduction of DOPAC level (data not shown). On the other hand, 5-day treatment of ZNS (1–100 μM) significantly increased DA/DOPA chrome level in CATH.a cells (Fig. 4).

Finally, we examined the effects of ZNS on excess cytosolic free DA-induced quinone formation by measuring quinoprotein levels in CATH.a cells after treatment with BH_4 (100 μM) and ketanserin (10 μM) with/without ZNS (1–100 μM) for 3 h. The quinoprotein levels in CATH.a cells co-treated with BH_4 and ketanserin for 3 h (which increase cytosolic free DA) were relatively higher than that in control at day 1 (Fig. 5), in agreement with a previous report (Choi et al., 2005). The simultaneous treatment of ZNS (1–100 μM) significantly and dose-dependently inhibited BH_4- and ketanserin-induced quinoprotein formation in the cells (Fig. 5).

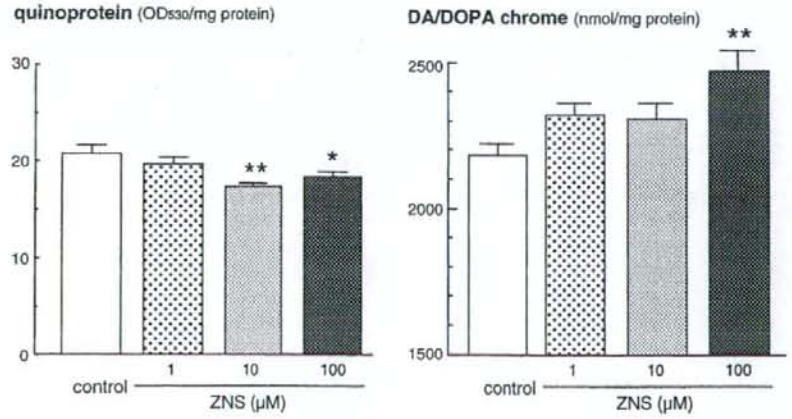

Fig. 4. Effects of long-term treatment of ZNS on quinoprotein and DA/DOPA chrome in dopaminergic CATH.a cells. After treatment with ZNS (1–100 μM) for 5 days, levels of quinoprotein ($n = 5$) and DA/DOPA chrome ($n = 6$) were measured in dopaminergic CATH.a cells, as indicated in Section 2. Data are mean ± S.E.M. $^{*}p < 0.05$, $^{**}p < 0.01$ compared with the control group.

4. Discussion

The main findings of this study are: (1) co-incubation of DA and ZNS in a cell-free system caused conversion of DA to stable melanin via formation of DA-semiquinone radicals and DA chrome; (2) long-term treatment with ZNS for 5 days decreased quinoprotein and increased DA/DOPA chromes in dopaminergic CATH.a cells; and (3) ZNS significantly inhibited quinoprotein formation induced by BH_4 and ketanserin that increase cytosolic free DA in the cells.

Long-term treatment of patients with PD by levodopa frequently causes various adverse effects including the wearing-off phenomenon, dyskinesia and psychiatric symptoms (Ahlskog and Muenter, 2001; Ogawa et al., 2005). However, long-term levodopa treatment-induced adverse effects that might be based on permanent neuronal network remodeling were seen specifically in PD patients but not in normal subjects or neurological diseases other than PD (Ogawa et al., 2005). Since the striatal damaged nerve terminal have too small DA pool to store DA at advanced stage of PD, repeated intermittent pulsatile levodopa stimulation results in free DA excess in the cytosol outside the synaptic vesicle (Sulzer et al., 2000; Sulzer and Zecca, 2000; Asanuma et al., 2003; Ogawa et al., 2005). The previous study revealed that repeated levodopa administration elevated striatal quinoprotein levels specifically on the parkinsonian side, not on the control side, of hemi-parkinsonian mice (Miyazaki et al., 2005). Therefore, the parkinsonian side-specific elevation of quinone generation may be due to excess amount of cytosolic DA outside the synaptic vesicles, which is easily oxidized to DA quinones in damaged dopaminergic nerve terminals after repeated levodopa treatment. In cultured dopaminergic cells, simultaneous treatment with ZNS dose-dependently suppressed BH_4- and ketanserin-induced quinoprotein formation via elevation of cytosolic free DA (Fig. 5), suggesting that ZNS has potent neuroprotective effects against neurotoxicity of DA quinone induced by excess amount of cytosolic DA outside the synaptic vesicles.

The protective effects of ZNS against levodopa-induced DA quinone toxicity in parkinsonian models may be based, in part, on its stabilizing effects against free DA and cytotoxic DA quinone; ZNS can convert free DA to melanin via the formation of DA-semiquinone radicals (Figs. 1 and 2) and subsequent intermediate DA chrome in the cell-free system (Fig. 3). This possible mechanism is also supported by the present results of long-term treatment with ZNS in cultured dopaminergic CATH.a cells. Long-term ZNS treatment in CATH.a cells for 5 days significantly decreased quinoprotein and increased DA/DOPA chromes (Fig. 4) with reduction of DOPAC (data not shown), suggesting that continuous ZNS exposure to DA-rich CATH.a cells promotes conversion of free DA and DA quinone to DA chrome, then to melanin. However, these effects do not seem to be exerted in a dose-dependent manner. Likewise relatively low doses of ZNS (25, 50 mg/day) rather than 100 mg/day significantly improved UPDRS Part III total score in the clinical trial (Murata et al., 2007), there may be optimal concentration range of ZNS to exert its stabilizing effects against DA quinones.

Several neuroprotective strategies have been proposed against DA quinone-induced cytotoxicity: (1) quenching excess free DA and DA quinone, (2) inhibiting quinone formation, and (3) enhancing intrinsic antioxidative system against DA quinone toxicity (Asanuma et al., 2004). Regarding quenching DA quinone, DA quinone can be scavenged by direct conjugation with some drugs, *e.g.*, thiol-containing compounds (*N*-acetylcyteine and dithiothreitol) (Offen et al., 1996) and DA agonists (pergolide and pramipexole) (Asanuma et al., 2005; Miyazaki et al., 2005). Furthermore, another possible method to quench DA quinone-induced cytotoxicity is the conversion of free DA and DA quinone to stable melanin. The final oxidized form of DA quinone, neuromelanin, exerts cytoprotective effects through its binding capacity to toxic metals (Zecca et al., 2003). Although large amount of neuromelanin with iron is reported to be potentially cytotoxic, physiological amount of neuromelanin is not toxic and rather cytoprotective with its high storage capacity for toxic metals in the substantia nigra (Gerlach et al., 2003; Zecca et al., 2003). This cytoprotective potency by stabilization of DA quinone has been clarified by our previous report that melanin-synthesizing enzyme tyrosinase ameliorates methamphetamine-induced neurotoxicity and quinoprotein formation *in vitro* and *in vivo* by its rapid conversion of DA quinone to melanin (Miyazaki et al., 2006). Also in the present study, we showed that ZNS can convert free DA to melanin via the formation of DA quinone and the intermediate DA chrome in the cell-free system. Therefore, these stabilizing effects of ZNS on free DA and DA quinone by the conversion to melanin may be one of the plausible mechanisms of its prevention against DA quinone-induced cytotoxicity.

ZNS is also known to scavenge hydroxyl radicals and nitric oxide radicals in a cell-free system (Mori et al., 1998) and inhibits lipid peroxidation and oxidative DNA damage in the rat brain (Komatsu et al., 2000). The general ROS such as hydroxyl radicals and nitric oxide radicals show widespread toxicity not only in DA neurons but also in other regions. Since the DA quinone is specifically generated from free cytosolic DA (Sulzer et al., 2000), the stabilizing effects of ZNS on free DA and cytotoxic DA quinone as dopaminergic neuron-specific oxidative stress may play a role in its preventing property against DA or levodopa-induced DA quinone toxicity, in addition to its scavenging activity against general ROS.

In conclusion, ZNS suppressed excess cytosolic free DA-induced quinone generation in dopaminergic cells. Furthermore, ZNS stabilized free DA and DA quinone as dopaminergic neuron-specific oxidative stress by the conversion to melanin. The stabilizing effects of ZNS against cytotoxic DA quinones may play a role in the efficacy of its adjunctive treatment to levodopa in parkinsonian patients.

Acknowledgments

This work was supported in part by Health and Labour Sciences Research Grants for Research on Measures for Intractable Diseases, for Research on Psychiatric and Neuro-